PROCESS-BASED NUMERICAL MODELING OF VEGETATED DUNE EROSION BY IRREGULAR WAVES

A Thesis

by

MATTHEW JAMES POWER

Submitted to the Office of Graduate and Professional Studies of
Texas A&M University
in partial fulfillment of the requirements for the degree of

MASTER OF SCIENCE

Chair of Committee,	Jens Figlus
Committee Members,	Russell Feagin
	Kuang-An Chang
Head of Department,	Sharath Girimaji

May 2019

Major Subject: Ocean Engineering

Copyright 2019 Matthew Power

ABSTRACT

Coastlines often have to be maintained through engineering practices to preserve coastal communities and environments and to limit damage from flooding during storm impact. As the expenses of coastal upkeep increase due to increasing near-shore human populations and climate change, cheaper and more environmentally conscious options are preferred. Vegetated dunes can provide such an option, whether naturally occurring, or engineered. The proper use of vegetation has been shown to reduce rates of dune erosion during wave impact. Unfortunately, information regarding vegetated dune application is sparse and quantification of the benefits of various vegetation strategies for erosion reduction is still limited. Morphodynamic changes of coastal profiles including sand dunes resulting from hydrodynamic forcing are usually simulated via process-based numerical models to assess beach nourishment and dune restoration design options. However, many of these models need to incorporate the vegetation effect on erosion in a simplified process parameterization which requires calibration with field and laboratory data.

The proposed work investigates the potential of the open-source 1D cross-shore depth-averaged morphodynamic model CSHORE to simulate erosion of vegetated dunes during elevated storm water levels and irregular wave impact. This was accomplished by adjusting various CSHORE parameters such as the spatially-varying bed friction factor and the substrate angle of repose, to match beach and dune profile evolution and hydrodynamic data obtained from a small-scale physical model wave flume experiment conducted with real sand and real vegetation (4 different morphotypes). The effect vegetation characteristics have on erosion and nearshore hydrodynamics will also be evaluated.

Results show that CSHORE is capable of simulating vegetated dune profile evolution during wave-induced erosion to some extent by adjusting model parameters, but it also becomes evident that a new subroutine specifically addressing the aboveground and belowground aspects of vegetation on dune erosion will be a necessary future model update. However, the extent of representing vegetation strictly as friction coefficients within CSHORE is bleak. On the other hand, the numerical model responded more appropriately to the inclusion of vegetation when the angle of repose was varied instead, indicating that higher vegetation characteristics (i.e. above-ground surface area, fine root mass, coarse root mass, stem rotational stiffness, and mycorrhizal population) can likely be represented as higher angles of repose within the dune area. Results from this thesis could assist in providing more cost-effective engineering guidelines for coastal engineers looking for ways to incorporate vegetated dune systems into their coastal protection strategies.

CONTRIBUTORS AND FUNDING RESOURCES

Contributors

This work was supported by a thesis committee consisting of Professors Jens Figlus and Kuang-An Chang of the Department of Ocean Engineering and Professor Russell Feagin of the Department of Ecosystem Science and Management.

Funding Sources

This work was made possible in part by graduate study fellowships from Texas A&M University and the American Bureau of Shipping. Its contents are solely the responsibility of the authors and do not necessarily represent the official views of the institutions.

TABLE OF CONTENTS

Page

LIST OF FIGURES

Page

LIST OF TABLES

Page

CHAPTER I

INTRODUCTION AND

LITERATURE REVIEW

Coastal zones are subjected to destructive erosion due to their proximity to the ocean, thus creating a need for protective measures. A potentially favorable method involves using vegetation to increase the erosion resistance of sand dunes. With knowledge of the quantitative role vegetation plays in reducing erosion limited, research must be conducted if engineering guidelines for incorporating vegetation into dune erosion reduction strategies are to be made. The method evaluated herein involves calibrating parameters within the cross-shore profile evolution numerical modeling software, CSHORE, to generate comparable effects to those produced by real vegetation (Kobayashi, 2013).

Approximately 10% of the world's population lives within ten meters of the sea level (McGranahan, Balk, & Anderson, 2007). Erosion due to wave action, especially during extreme storm events, continually creates the need for coastal protection measures. These measures usually include the construction of hard structures, such as sea walls (Figure 1.1a), to prevent wave-induced damages. Methods for restoring eroded coastlines, such as beach nourishment (Figure 1.1b), are also frequently required.

Construction of hard structures and beach nourishment are expensive means for protecting shorelines. According to the American Shore & Beach Preservation Association (ASBPA), beach nourishment alone has cost the United States $6.2 billion as of 2018 ("National Beach Nourishment Database," 2019). An alternative approach to protecting the coastline involves Engineering with

Nature® (EWN), which is a design philosophy seeking to systematically integrate natural and nature-based features (NNBF) for coastal hazard risk-reduction as well as social, environmental, and economic considerations at every stage of a project (Strelzoff, 2019). This philosophy results in coastal protection schemes in addition to coastal risk-reduction measures that rely on natural features such as vegetated sand dunes and salt marshes. EWN is currently limited by the scarce amount of quantitative knowledge regarding the role vegetation plays in coastal protection. The proposed thesis seeks to fill in some of the gaps of this knowledge by seeking ways to represent the influence varied morphotypes of coastal vegetation have on erosion and nearshore hydrodynamics.

Figure 1.1: Three methods to reduce the risk for flooding and flood-related damages along coastlines. The Galveston Seawall is shown in (a) (Snyder, 2017). (b) shows sand being pumped from offshore onto an eroded beach for a beach nourishment project, image courtesy of SCEhardt. (c) displays a vegetated sand dune (Feagin et al., 2015)

The role of plants in coastal dune morphology has been known for over 100 years (Cowles, 1899), but specific details of their role would not be investigated until after the Bhola Cyclone devastated Bangladesh, where vegetation played a role in protecting certain areas from damages (Fosberg & Chapman, 1971). Even then, information on the interaction between dune vegetation

and wave action is lacking (Stallins & Parker, 2003). Modern experiments usually involve studying the interaction between simulated vegetation and waves as opposed to real vegetation, or strictly use only one species (Silva, Martínez, Odériz, Mendoza, & Feagin, 2016). Some studies modeled vegetation as wooden dowels (Kobayashi, Gralher, & Do, 2013) and coir fibers (Bryant, Bryant, & Grzegorzewski, 2017) while others have used synthetic materials. Few experiments have involved multiple species of vegetation, and even fewer have explored the link between dune morphology and different vegetation characteristics (e.g. below-ground root mass, above-ground area coverage, stem rigidity).

Many numerical models have been developed for simulating shoreline evolution of coastal zones subject to various hydrodynamic conditions. These conditions can range from wakes of passing ships to extreme storm event conditions. In general, most numerical cross-shore evolution models are sensitive to offshore sand bars, and often times irregular waves unnaturally lessen the profile slope after wave impact. Three models in particular (NPM,HR; UNIBEST,DH; and LITCROSS,DHI) have too large of cross-shore sediment transport gradients immediately onshore of wave breaking (J. A. Roelvink & Brøker, 1993). Some numerical models like SBEACH (Storm-induced Beach Change) can model bar formation and migration produced by breaking waves (Larson, Kraus, & Byrnes, 1990). Another popular model, XBEACH (extreme beach behavior), is especially adept at simulating dune overwash and breaching during extreme storm events (D. Roelvink et al., 2009). For this thesis, CSHORE (Cross-Shore Numerical Model), was utilized to simulate the shoreline evolution of a vegetated, experimental sand dune. A major strength of CSHORE lies in its utilization of a probabilistic model for wave runup, which is significantly more computationally efficient than wave-resolving models used by many other cross-shore numerical models.

This thesis involves processing profile-evolution data collected during work performed by Sigren *et al*, in which the role vegetation characteristics play in effecting dune morphology was studied. His experiment involved impacting a vegetated shoreline with multiple 210-second-long wave runs. Both the profile evolution and hydrodynamic properties were measured. For this thesis, CSHORE was used to simulate the measured morphodynamic evolution of the beach and dune profile. Major discrepancies between the vegetated experimental profile and the non-vegetated numerical profile were resolved by calibrating relevant CSHORE parameters, most important of which were speculated to be the bed friction coefficients in the nearshore area and angles of repose. The parameters that produce best-matching numerical profiles to the experimental profiles were then correlated to their matching vegetation. The results are expected to assist in producing guidelines for incorporating specific types of vegetation in CSHORE.

CHAPTER II

RESEARCH QUESTIONS

AND HYPOTHESES

The purpose of this research is to assess the feasibility of modeling different vegetation morphotypes within CSHORE as bed friction coefficients and angles of repose of the substrate. It was seen from Sigren's research that vegetation alters the morphodynamics of the shoreline. In particular, above-ground surface area and below-ground root mass reduced erosion and increased the steepness of the dune scarp. Above-ground traits such as leaves and stem stiffness was shown to decrease the turbulent kinetic energy within the swash zone by increasing flow resistance, which decreases disturbance of sediment; one way to simulate the above-ground characteristics is through altered bed friction coefficients. Below-ground root mass held sediments together, which both reduced erosion and influenced the steepness of the scarp; this effect could potentially be represented within CSHORE by altering the maximum allowed angle of repose of the sediment.

As of this research, there have been few attempts to represent the influence vegetation has on morphodynamics and hydrodynamics within numerical models. The information presented herein naturally leads to Research Question I:

Research Question I: To what extent can the effects of root biomass, above-ground area coverage, and stem rigidity of vegetation on the evolution of dune profiles under wave attack be simulated with the numerical morphodynamical model, CSHORE?

The hypothesis for Research Question 1 is as follows:

Hypothesis I: Vegetation characteristics can be reliably represented as modified bed friction coefficients at the location of vegetation in the profile or as an increased angle of repose within CSHORE.

CHAPTER III

PHYSICAL MODEL

WAVE FLUME EXPERIMENT

3.1 Wave Flume

Prior to this thesis, physical model wave flume experiments were performed in the TAMUG moveable-bed wave flume (Sigren, 2017). The flume is shown in Figure 3.1. This wave flume houses an experimental shoreline comprised of real sand, which can be subjected to various wave conditions generated by a flap-type wave maker. Waves generated by the wave maker were formulated using the Joint North Sea Wave Observation Project (JONSWAP) spectrum, which is based on storms occurring in the North Sea (Hasselmann et al., 1973). Within the flume, a cross-section of a vegetated shoreline was modeled by introducing samples of four types of vegetation into the swash zone: *Sporobolis Virginicus (SV), Sesuvium Portulacastrum (SP), Rayjacksonia Phyllocephala (RP), and Panicum Amarum (PA).* Mounted on top of the wave flume is a laser line scanner for measuring sand dune profile evolution. The profile of the shoreline was measured both before and after wave runs were performed.

Figure 3.1: The TAMUG moveable-bed wave flume (Sigren, 2017)

Capacitance wave gauges (WG) are mounted along the length of the flume in nine separate locations. These wave gauges measure water surface elevation. The sand composing the experimental shoreline sits atop a plywood platform. Acoustic Doppler Velocimeters (ADV) are mounted at wave gauge locations within the swash and collision regimes. These ADVs measure the velocity of suspended sediment particles via an acoustic ping. Vegetation can be supplanted into the wave flume at various locations along the profile. The vegetation was placed within the swash zone immediately in front of the dune, as seen in Figure 3.2.

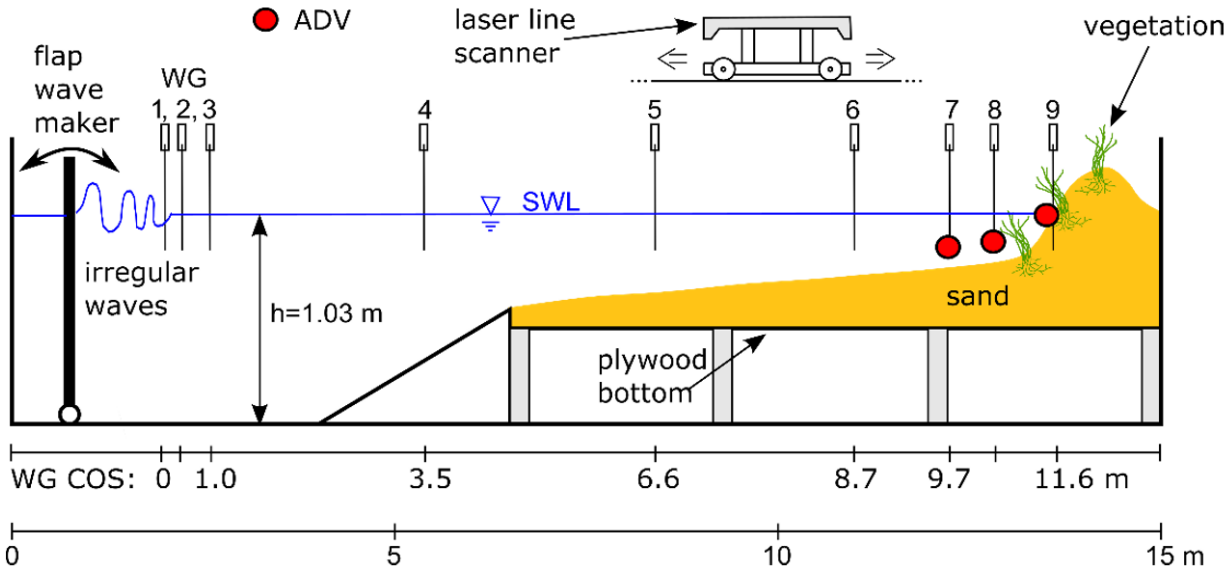

Figure 3.2: A schematic of the TAMUG moveable bed wave flume (Figlus, Sigren, Power, & Armitage, 2017). The wave gauge locations are shown along the line labeled, "WG COS:" The first wave gauge is placed at x=0.

3.2 Vegetation

Four species of vegetation were used for the experiments (Sigren, 2017). The species are as follows:

- *Sporobolis Virginicus (Figure 3.3a):* A short dune grass commonly found along the Texas coastline.
- *Panicum Amarum (b):* A tall dune grass characterized by its tall, rigid stem that can grow to be a meter in height. Its root system is dense and adventitious.
- *Sesuvium Portulacastrum (c):* A spreading vine found on and near dunes. It rarely grows more than 5 cm off the ground. The species has a taproot structure with moderately dense finer roots spreading from the taproot.
- *Rayjacksonia Phyllocephala (d):* A dune shrub that can grow up to 50 cm in height. For this experiment, seedlings of height 5-10 cm were used.

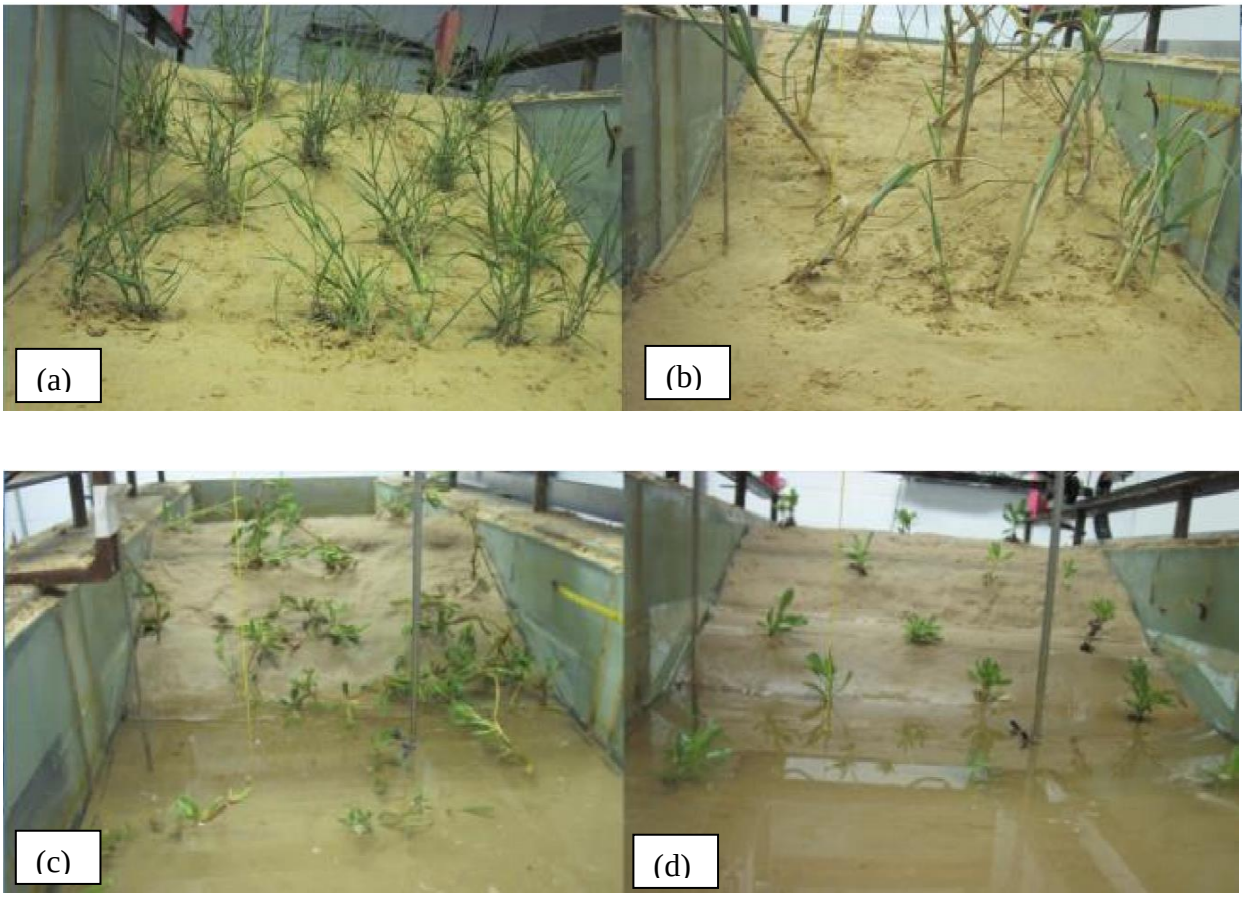

Figure 3.3: The four species of vegetation used in the experiment. Each species was chosen based on the measurable differences between each other as well as their relevance to the Texas coastal ecosystem. Measurable difference can include above-ground area coverage, below-ground root mass, stem rigidity, and type of root structure among others.

3.3 Results

The results of the experiment indicated that both above and below ground properties of plants contributed to dune erosion resistance during wave impact. Specifically, aboveground plant surface area was the key factor in reducing swash flow velocity, turbulent kinetic energy, and wave reflection. Fine root mass was responsible for increasing sediment shear strength (Sigren, 2017). Interestingly, inspection of the results shows that root-biomass also had the effect of increasing the slope of dune scarping, which shows that below-ground properties of plants increases the angle of repose of the sediment.

The relationship between the major vegetation parameters and morphological changes is shown in Figure 3.4. Two star plots are used in the figure to help illustrate the relations. The green star plot provides a qualitative picture of the chief characteristics of vegetation considered and their magnitude relative to each other, which are:

- Fine root biomass (FR)
- Coarse root biomass (CR)
- Aboveground swash zone surface area of stems and leaves (SA)
- Stem rotational stiffness (RS)
- Mycorrhizal fungi colonization (MC).

Arbuscular mycorrhizal fungi are microbial communities present within and around the root system of vegetation, and are responsible for helping the plants bind together grains of sand by increasing soil aggregation and shear strength. The brown star plot illustrates the sand dune morphological response. The parameters are:

- Eroded Volume (E)
- Scarp Retreat (R_s)
- Cross-Shore Centroid Shift (S).

Finally, the profile plots show the change in shoreline after exposure to increments of successive wave impact. Black plots indicate the initial profile prior to any wave impact while the warmer colors indicate longer exposure times, with the maximum exposure time being 2520 seconds of wave impact. Among other results, the takeaways relevant to the present research are:

- Offshore shift of sediment was reduced by vegetation containing more fine roots and leaves/stems (aboveground surface area)

- Dune scarp retreat was hindered by fine roots and aboveground surface area
- Eroded volume of sediment was negatively related to fine root mass and aboveground plant surface area
- Root mass played a significant role in increasing the slope of the dunes, implying that the angle of repose is altered by below-ground vegetation features.

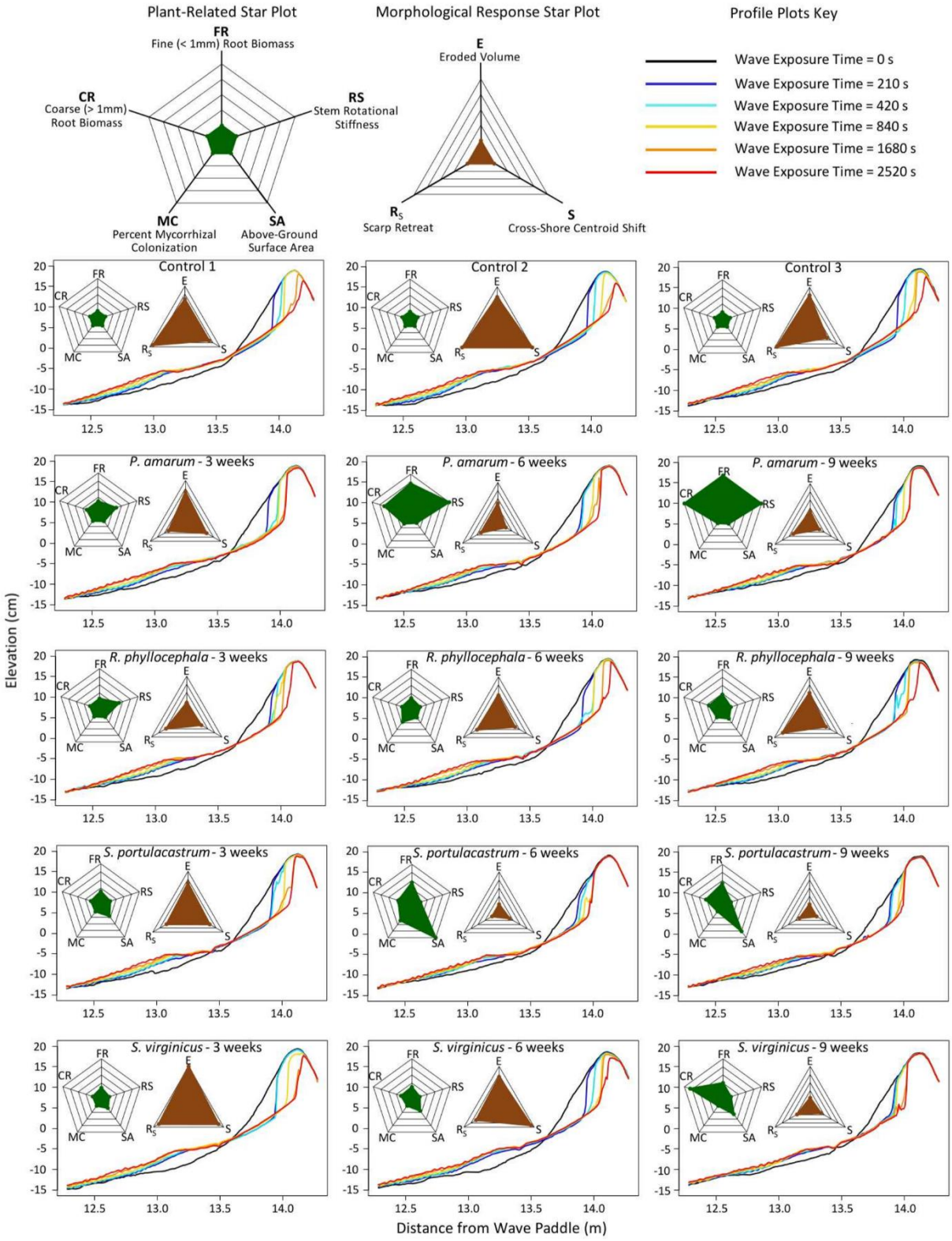

Figure 3.4: The relationship between vegetation parameters and dune morphology changes for all tests (Sigren, 2017).

CHAPTER IV

NUMERICAL MODEL: CSHORE

4.1 Overview

CSHORE is a 1D, process-based, cross-shore numerical shoreline evolution and hydrodynamic model developed by Kobayashi and funded in large part by the Army Corps of Engineers for the purpose of providing a simple yet robust model for predicting morphological changes and nearshore hydrodynamics caused by wave-shore interactions (Kobayashi, 2013). One of the major strengths of the model lies in its ability to produce results within seconds. The model is comprised of:

- A combined wave and current model, cross-shore and longshore momentum, wave energy and action, and roller energy equations
- Combination of linear wave theory and shallow water wave equations, with the two only slightly overlapping
- A sediment transport model encompassing both suspended sand and bedload
- A permeable layer model
- Consideration of irregular wave runup
- A probabilistic model for predicting wave overwash that is satisfied for alternating wet-dry zone conditions on either impermeable or permeable bottoms.

The model is limited to cases of time-averaged continuity, alongshore uniformity, and uniform sediment characterized by a mean diameter (d_{50}).

CSHORE can be run as an executable file on any computer. The only requirement is to place an "infile" containing all necessary and properly formatted input parameters within the same folder as the CSHORE executable. Input parameters for CSHORE include an initial profile (with z=0 as the still water level), wave characteristics (root-mean-square wave height (H_{rms}), peak wave period (T_p)), sediment characteristics, and bed frictional coefficients (f_b) for each cross-shore location. The relevant CSHORE output within the context of this thesis includes profile evolutions at multiple time intervals.

4.2 Numerical Modeling of Hydrodynamics

For x and z being the horizontal and vertical axis respectively, CSHORE generates hydrodynamic conditions for a given set of parameters defined at the seaward boundary x=0 with a still water level (SWL) at z=0. Given these wave conditions, the model uses linear wave and current theory to calculate wave refraction, which predicts spatial variations of H_{rms} and incident wave angle (θ) at each cross-shore location via the dispersion relation (Dalrymple & Kirby, 1988):

$$\omega^2 = kgtanh(k\bar{h}); \omega_p = \omega + \frac{k\left(Q_x \cos(\theta) + Q_y \sin(\theta)\right)}{\bar{h}} \quad (4.1)$$

The parameters are:

- ω: Intrinsic angular frequency
- k: Wave number
- g: Gravitational acceleration
- $\bar{h}$: Time averaged mean water depth
- ω_p: Absolute angular frequency given by $\omega_p = \frac{2\pi}{T_p}$
- T_p: Peak wave period

- $Q_x \; and \; Q_y$: Time averaged volume flux per unit width in the x and y directions, where x is the cross-shore coordinate and y is the alongshore coordinate.

The time averaged momentum and continuity equations are evaluated to compute the mean water depth ($\bar{h}$) and current velocities in the x and z directions respectively, $\overline{U}$ and $\overline{V}$ (Phillips, 1977):

$$\frac{\partial}{\partial x}(Q_x) + \frac{\partial}{\partial y}(Q_y) = 0 \quad (4.2)$$

Where,

$$Q_x = \bar{h}\overline{U} + \frac{g\sigma_\eta^2}{C}\cos(\theta) + q_r \cos(\theta) \quad (4.3)$$

$$Q_y = \bar{h}\overline{V} + \frac{g\sigma_\eta^2}{C}\sin(\theta) + q_r \sin(\theta) \quad (4.4)$$

And the variables are:

- C: Phase speed
- σ_η: Standard deviation of the free surface elevation, η
- θ: Angle from the normal to the shoreline
- q_r: Volume flux of roller at the breaking wave.

4.3 Numerical Modeling of Shoreline Evolution

The previously mentioned combined wave and current model produce spatial variations of the hydrodynamics used in the sediment transport model described herein. CSHORE calculates the change in bed elevation by observing the continuity equation of sediment transportation:

$$(1 - n_p)\frac{\partial z_b}{\partial t} + \frac{\partial q_x}{\partial x} + \frac{\partial q_y}{\partial y} = 0 \quad (4.6)$$

Where,

- z_b: Bed elevation
- n_p: Porosity of bottom sediment
- t: Time coordinate
- x: Cross-shore coordinate
- y: Alongshore coordinate
- q_x: Cross-shore total sediment transport rate
- q_y: Alongshore total sediment transport rate.

For the present thesis, alongshore uniformity is assumed, so the third term of the equation drops out, reducing the equation to:

$$\left(1 - n_p\right)\frac{\partial z_b}{\partial t} + \frac{\partial q_x}{\partial x} = 0 \quad (4.7)$$

Friction and the angle of repose come into play through cross-shore total sediment transport (q_x), which is broken into two components:

$$q_x = q_{sx} + q_{bx} \quad (4.8)$$

Here, q_{sx} is the cross-shore suspended sediment transport rate, defined by:

$$q_{sx} = \alpha_x \bar{U} V_s \quad (4.9)$$

And the cross-shore bedload sediment transport rate is defined by:

$$q_{bx} = B_b \overline{(U^2 + V^2)U} \quad (4.10)$$

Where,

- α_x: A parameter that depends on the empirical suspended load parameter, cross-shore bottom slope, and the angle of internal friction of the sand, ϕ
- U: Cross-shore velocity
- V: Alongshore velocity
- $\overline{U}$: Time averaged, depth averaged cross-shore velocity
- V_s: Suspended sediment volume
- q_{bx}: Cross-shore bed sediment transport rate
- B_b: An empirical parameter.

Ultimately, bed friction coefficients (f_b) influence both the bedload sediment transport and suspended sediment transport through their influence on the probability of sediment movement (P_b), which is controlled in large part by the shear stress exerted on the bed by a moving fluid,

$$\tau_b' = 0.5\rho f_b U_a^2 \quad (4.11)$$

Where $U_a = \sqrt{U^2 + V^2}$.

CSHORE solves the continuity equation for sediment transport through an explicit Lax-Wendroff numerical scheme to obtain the new bottom elevation at each successive time increment. This calculation is repeated for each time increment throughout a test. For example, a test lasting ten seconds with time increments of 1/10th of a second would require a total of 100 calculations before the solution is found (Kobayashi, 2013).

CHAPTER V

DATA ANALYSIS METHODS

5.1 Measured Beach and Dune Profiles

To answer Research Question I and verify Hypothesis I, the results of the five separate experiments performed within the TAMUG moveable bed wave flume were processed, then compared with results from CSHORE. The results of four trials, each composed of different vegetation morphotypes, were compared against a trial without vegetation, designated as the control trial. Figure 5.1 shows the relationship between tests and trials. For each test, the initial and final profiles were measured.

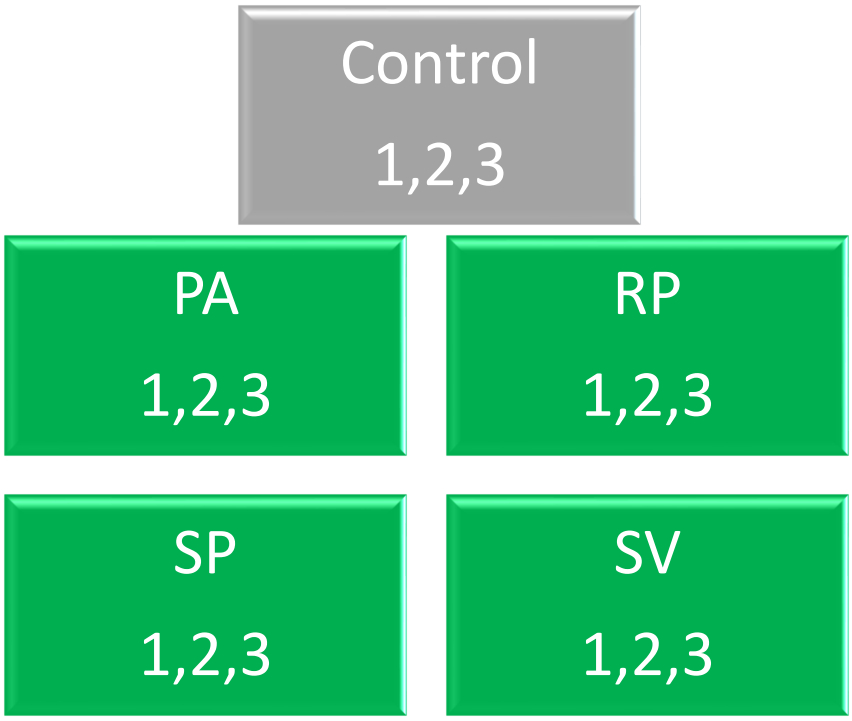

Figure 5.1: Illustration of the experiment performed by Sigren. The boxes represent the trials (Control, PA, RP, SP, SV) and the contained tests (1,2,3). In total, 15 tests were performed within 5 trials. Each test involved 12 wave bursts, each of which lasted 210 seconds.

The first of the five trials involved impacting a non-vegetated shoreline with twelve bursts of waves each lasting 210 seconds. The profile elevation was measured at six points in time, the first of which was prior to any wave runs. Each experiment involved three tests. For the control trials, each test was identical, and contained no vegetation. For the vegetated trials, each test involved different stages of vegetation maturity, with the first test corresponding to three-week maturity, the second to six weeks, and the final to nine weeks of maturity. As the plants mature, the characteristics governing its influence on sediment transportation, such as root biomass, aboveground surface area, and stem rigidity, generally increase. The initial elevations were imported into CSHORE and smoothed prior to calculations. After CSHORE performs calculations, the results are then compared to the final measured profiles from every test, and the discrepancies between the two are calculated.

5.2 CSHORE-Simulated Profiles

Relevant parameters within CSHORE were calibrated to produce a shoreline more closely resembling the sand dune profiles of the experiments. The first key parameter is the bed friction coefficient. This parameter is directly proportional to the shear stress induced by waves on sand particles, thus making it a primary inhibitor of sediment transport. Each cross-shore location has a unique friction coefficient, which can be calibrated to influence sediment transport at a desired location. The results of the experiment were examined for each vegetation morphotype and maturity type to determine a trend between specific vegetation and friction coefficients in the swash zone. The experimental and CSHORE profile outputs appear as shown in Figure 5.2. The front of the dune is defined as the location where the initial measured dune profile intersects the final measured dune profile (where erosion stops and accretion begins).

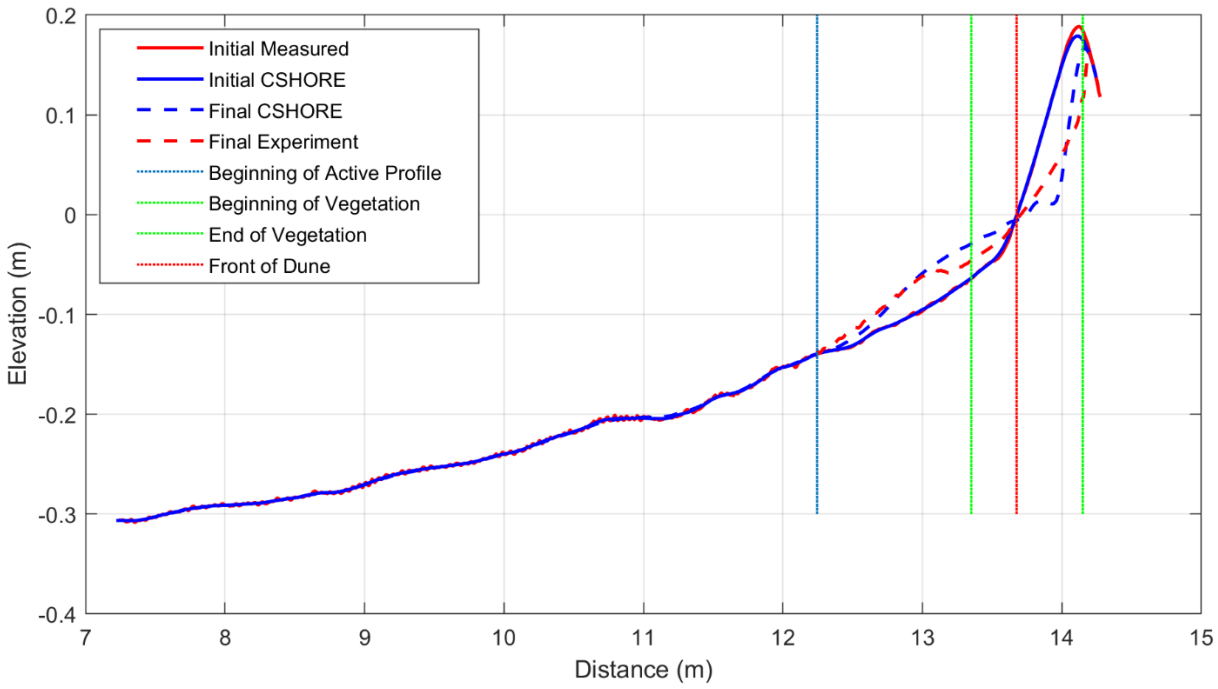

Figure 5.2: Cross-shore profile evolutions. Experimental profiles are defined in solid and dashed red while CSHORE profiles are solid and dashed blue. Solid and dashed lines indicate initial and final profiles respectively. The vertical, dotted blue line indicates the beginning of the active profile. The dotted green lines indicate the beginning and end of the vegetation. The dotted, vertical red line indicates the front of the sand dune, which is where scarp retreat begins.

For the experiment, three zones along the profile are examined separately. These zones and their cross-shore boundaries are detailed in Table 5.1. Figure 5.3 shows each of these profiles and their cross-shore boundaries. The boundaries were selected based on their relevance to the present research, and include:

- Active Profile (APr): Cross-shore locations where non-negligible sediment movement occurs
- Vegetated Profile (VPr): Cross-shore locations where vegetation was placed for the physical experiments
- Scarped Profile (SPr): Cross-shore locations where scarping occurs. In other words, the location between the front face of the dune and the shoreward end of the profile.

Table 5.1: Seaward and landward boundaries of the profiles processed through data analysis.

	Seaward Boundary (m)	Shoreward Boundary (m)
Active Profile (APr)	12.235	14.255
Vegetated Profile (VPr)	13.345	14.145
Scarped Profile (SPr)	13.675	14.255

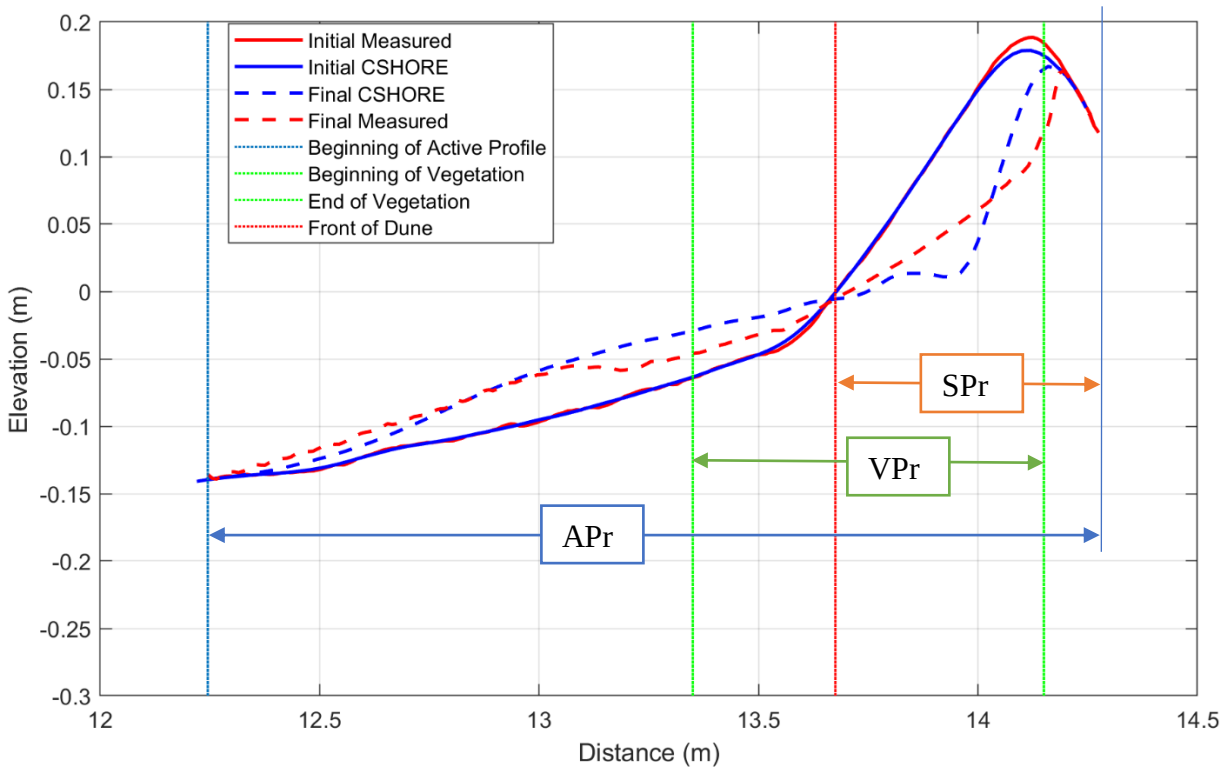

Figure 5.3: The zones where calculations were performed. The zones correspond to the active profile (APr), vegetated profile (VPr), and scarped profile (SPr) respectively.

After examining the experimental results for the profile evolution, CSHORE was run for the same initial profile, wave conditions, and time span as in the experiments. The resulting profile elevations were compared to those of the experiment. As will be shown in section 5.5, specific variables were fine-tuned to produce the best-match profile within CSHORE.

MATLAB® was utilized to perform data analysis and comparison of the experimental and numerical data. Evaluating the accuracy of the CSHORE results involved taking the root-mean-

square and standard deviation (separately) of the difference between the CSHORE and measured experimental results within zones APr, VPr, and SPr respectively, the equations of which are as follows:

$$STD = \sqrt{\frac{\sum_{i=1}^{N}\left(d_i - \bar{d}\right)^2}{N-1}} \quad (5.1)$$

$$RMS = \sqrt{\frac{\sum_{i=1}^{N} d_i^2}{N}} \quad (5.2)$$

Where d_i is the difference between the CSHORE profile elevation and measured profile elevation at each cross-shore location:

$$d_i = (d_c)_i - (d_m)_i \quad (5.3)$$

The parameters are as follows:

- N: Number of data points
- $(d_c)_i$: Depth of the CSHORE simulated elevation at each cross-shore location
- $(d_m)_i$: Depth of measured profile at each cross-shore location.

The resulting accuracies quantify the difference between the morphological output of CSHORE versus the experiment. Smaller rms and std values indicate higher accuracy since this means the differences between the profiles at each location are small. The only formulaic difference between rms and std is that the latter subtracts the mean of the differences between the CSHORE and measured results prior to squaring the data points. Thus, similar rms and std values indicate that the mean of the differences between CSHORE and measured data approach zero.

Another method of assessing the accuracy involved taking the integral of the differences between CSHORE and measured data. This method was abandoned since it described how much sediment leaves or enters the system without revealing anything about the geometry of the results, while std and rms give a general description of how different the geometries are relative to each other.

A histogram visualizes the spread of data (Figure 5.4b). Most values should be at or near zero if the result is accurate. To quantify the similarity of the two profiles, the standard deviation and root-mean-square are then calculated. The lower the standard deviation and root-mean-square, the more similar the profiles. The default value for $\tan(\phi)$ was chosen to be 0.63 since it is also consistent with that measured on sandy coastlines (Bailard, 1981).

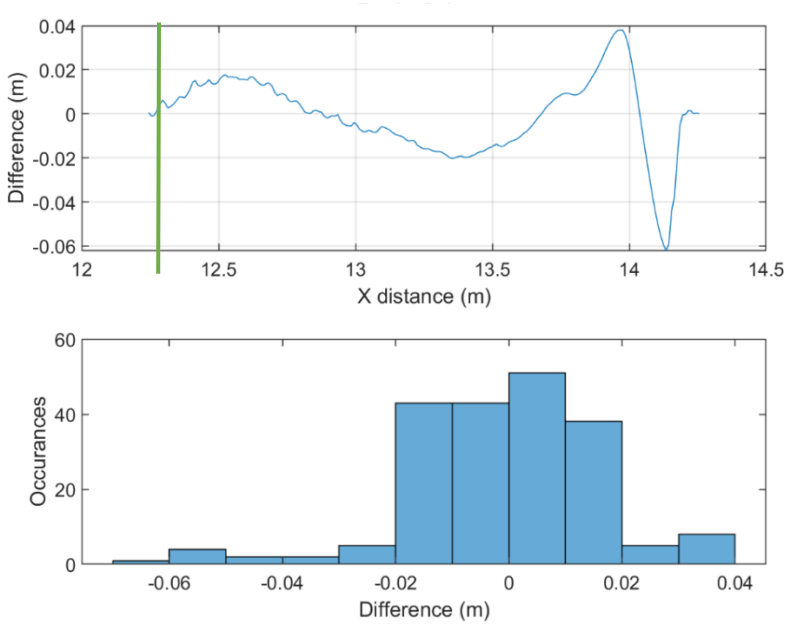

Figure 5.4: (a) Example of the difference between the experimental and CSHORE profile elevations past the beginning of the active profile (indicated by the green line). (b) Histogram of the graph in (a).

5.4 CSHORE-Input Parameters

The CSHORE program is an executable file that simply requires an infile to run. This infile contains binary case switches for different environmental conditions and subroutines, hydrodynamics, sediment characteristics, and shoreline elevations. This section discusses each of the cases and parameters used for performing the simulations (Kobayashi, 2013). The Appendix provides an infile for control trial C1.

Figure 5.5 shows an example of the primary input of an infile. The parameters within the red box are binary case switches which determine the type of simulation to run. The cases that were used for this experiment are:

- IPROFL: Profile elevations are calculated and stored
- ISEDAV: Limited sediment supply, meaning that no additional sediment is introduced to the system
- IOVER: Includes calculations for wave overtopping of the sand dune (if the hydrodynamic parameters predict it)
- IROLL: Includes roller effects in the wet zone.

Case switches that were turned off include calculations for wave-generating wind effects, tidal effects, wave and current interactions, water infiltration through the sand dune, ponding within runnels on the profile, standing waves or wave transmission in the landward wet zone of the dune, and permeability of the dune profile.

The variables in the blue box mainly have to do with sediment characteristics, and are as follows:

- DX (m): Cross-shore grid spacing
- GAMMA: Empirical breaker ratio parameter, obtained from the physical experiments

- D50 (mm): Median sediment diameter, obtained from the physical experiments
- WF (m/s): The sediment fall velocity, calculated using a sediment fall velocity Matlab code (Ruiz, 2007)
- SG: Specific gravity of the sediment, obtained from the physical experiments
- EFFB: Suspension efficiency due to breaking wave
- EFFF: Suspension efficiency due to bottom friction
- SLP: Suspended load parameter
- SLPOT: Suspended load parameter associated with the wave overtopping rate
- BLP: Bedload parameter
- TANPHI: Slope of the angle of repose of the sediment. The default values is 0.63, which is consistent with sandy shorelines (Bailard, 1981).

The values for the parameters EFFB and EFFF were chosen according to what was most accurate for trials C1 and C2. Accuracy was determined by taking the standard deviation of the difference between the final measured and CSHORE profiles for the entire cross-shore profile. The same process was used to determine SLP, SLPOT, and BLP. All of the chosen values for these five parameters lay within the range of calibrated values specified by Kobayashi.

The green box includes hydrodynamic parameters. The first three lines contain:

- ILAB: Specifies whether or not the specified hydrodynamic conditions were generated in a laboratory setting, which implies that the input wave and water level data are to be read together
- NWAVE: The number of sequential waves at x=0 where x is the cross-shore coordinate at which the waves are generated

- NSURG: The number of water levels at the seaward boundary of x=0.

The first column below NSURG is the morphological time in seconds. The second column is the peak wave period during the time specified in the first column, which is calculated from the laboratory hydrodynamics. The third column is the root-mean-square wave height calculated from the laboratory hydrodynamics. The final three columns are the wave setup, still water level above datum, and incident wave angle respectively; each of the latter three parameters are zero.

The final, yellow box contains the initial shoreline cross-shore locations, profile elevations, and friction coefficients. The parameters NBINP and NPINP specify the number of points describing the cross-shore profile elevation and impermeable boundary respectively. In Figure 5.5, NPINP is specifying that the final seven rows following the profile elevation describe the elevation of an impermeable layer on which the cross-shore profile rests. This boundary cannot be altered by wave action. A friction coefficient of 0.02 was chosen as the default value to be applied to the entire profile; the value is a standard value for sandy, impermeable beaches with smooth slopes (Pietropaolo, Kobayashi, & Melby, 2012).

```
1                                                   -> IPROFL
1                                                   -> ISEDAV
0                                                   -> IPERM
1                                                   -> IOVER
0                                                   -> IWTRAN
0                                                   -> IPOND
0                                                   -> INFILT
0                                                   -> IWCINT
1                                                   -> IROLL
0                                                   -> IWIND
0                                                   -> ITIDE
0.02                                                -> DX
0.6000                                              -> GAMMA
0.1520      0.0110      2.6500                      -> D50,WF,SG
0.0038      0.0060      0.1800      0.3000          -> EFFB,EFFF,SLP,SLPOT
0.95        0.0050                                  -> TANPHI,BLP
0.0200                                              -> RWH
1           -> ILAB
12          -> NWAVE
12          -> NSURGE
209.95       1.8696     0.065282    0           0           0
419.9        1.8696     0.064167    0           0           0
629.85       1.8696     0.064122    0           0           0
839.8        1.8696     0.064041    0           0           0
1049.75      1.8696     0.06388     0           0           0
1259.7       1.8696     0.063486    0           0           0
1469.65      1.8696     0.064469    0           0           0
1679.6       1.8696     0.063943    0           0           0
1889.55      1.8696     0.061756    0           0           0
2099.5       1.8696     0.062271    0           0           0
2309.45      1.9422     0.062448    0           0           0
2519.4       1.9422     0.061953    0           0           0
710                                                 -> NBINP
7                                                   -> NPINP
0           -0.912      0.02
1.1766      -0.912      0.02
1.595       -0.809      0.02
3.35        -0.377      0.02
```

Figure 5.5: Example of the inputs for an infile. The different colored boxes represent: (red) binary case switches; (blue) sediment characteristics; (green) hydrodynamic parameters; (yellow) cross-shore profile elevation and friction coefficients.

CHAPTER VI

RESULTS AND DISCUSSION

6.1 CSHORE-Experiment Similarity by Varying Friction Coefficients f_b

6.1.1 Results

This section examines the results of varying friction coefficients within CSHORE. The following figures and tables demonstrate to what degree variation of friction coefficients has on the accuracy of the numerical model. The friction coefficients within the vegetated profile were varied from $0.01 < f_b < 0.1$ in increments of 0.005. Figure 6.1 shows an example of the change in error with respect to varied friction coefficients for every trial. In particular, the figure is showing the rms error for the active profile.

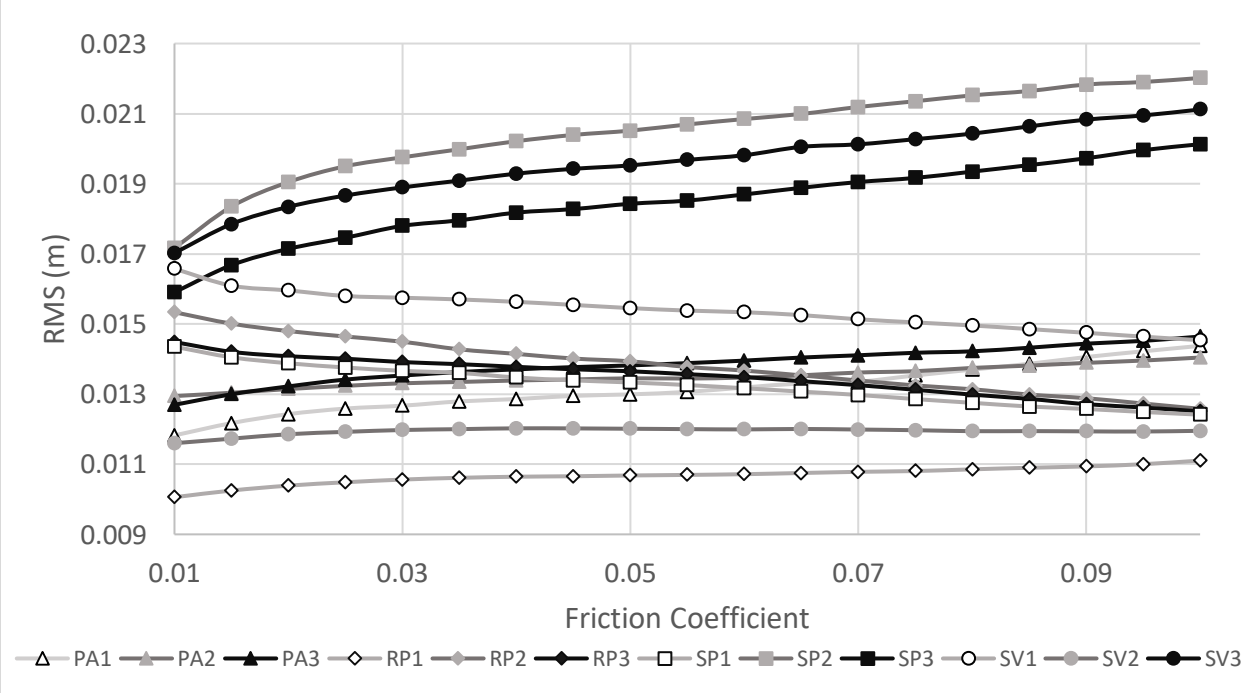

Figure 6.1: Example of the change in rms due to variation of f_b. A decrease in RMS indicates an increase in accuracy. As can be seen, there exists a friction coefficient at which each trial has a minimum rms error.

Friction coefficients corresponding to minimum rms and std errors were found for every trial. The results of this analysis for the active profile are shown in Figures 6.2 (rms) and 6.3 (std). The corresponding minimum values are shown in Tables 6.1 and 6.2 respectively.

Table 6.1: The initial rms error values (prior to varying friction coefficients) and the final rms error for APr.

APr	PA1	PA2	PA3	RP1	RP2	RP3	SP1	SP2	SP3	SV1	SV2	SV3
Initial (m)	0.0124	0.0131	0.0132	0.0104	0.0148	0.0141	0.0139	0.0190	0.0171	0.0160	0.0119	0.0183
Final (m)	0.0118	0.0129	0.0127	0.0101	0.0126	0.0125	0.0124	0.0172	0.0159	0.0145	0.0116	0.0170
fb	**0.01**	**0.01**	**0.01**	**0.01**	**0.1**	**0.1**	**0.1**	**0.01**	**0.01**	**0.1**	**0.01**	**0.01**

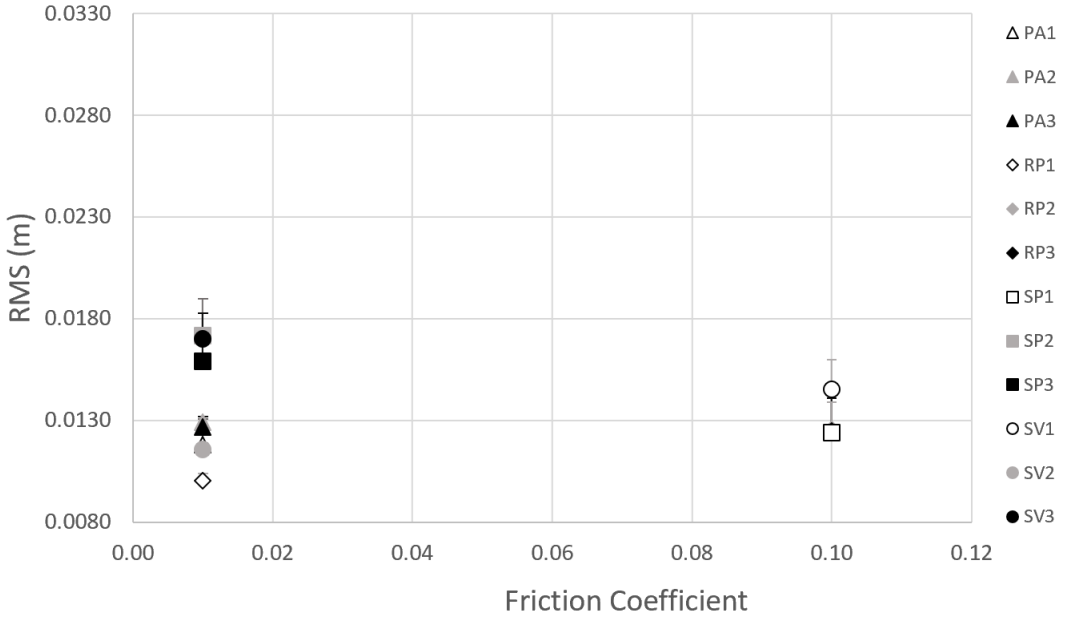

Figure 6.2: The minimum rms errors and the corresponding friction coefficients for every vegetated trial. The error bars indicate what the initial error was for each trial when a default friction coefficient of 0.02 was used. The profile zone is APr.

Table 6.2: The initial std error values (prior to varying friction coefficients) and the final std error for APr.

APr	PA1	PA2	PA3	RP1	RP2	RP3	SP1	SP2	SP3	SV1	SV2	SV3
Initial (m)	0.0120	0.0120	0.0123	0.0103	0.0141	0.0132	0.0133	0.0189	0.0170	0.0153	0.0117	0.0181
Final (m)	0.0114	0.0117	0.0117	0.0099	0.0118	0.0116	0.0118	0.0170	0.0157	0.0138	0.0114	0.0168
fb	**0.01**	**0.01**	**0.01**	**0.01**	**0.1**	**0.1**	**0.1**	**0.01**	**0.01**	**0.1**	**0.01**	**0.01**

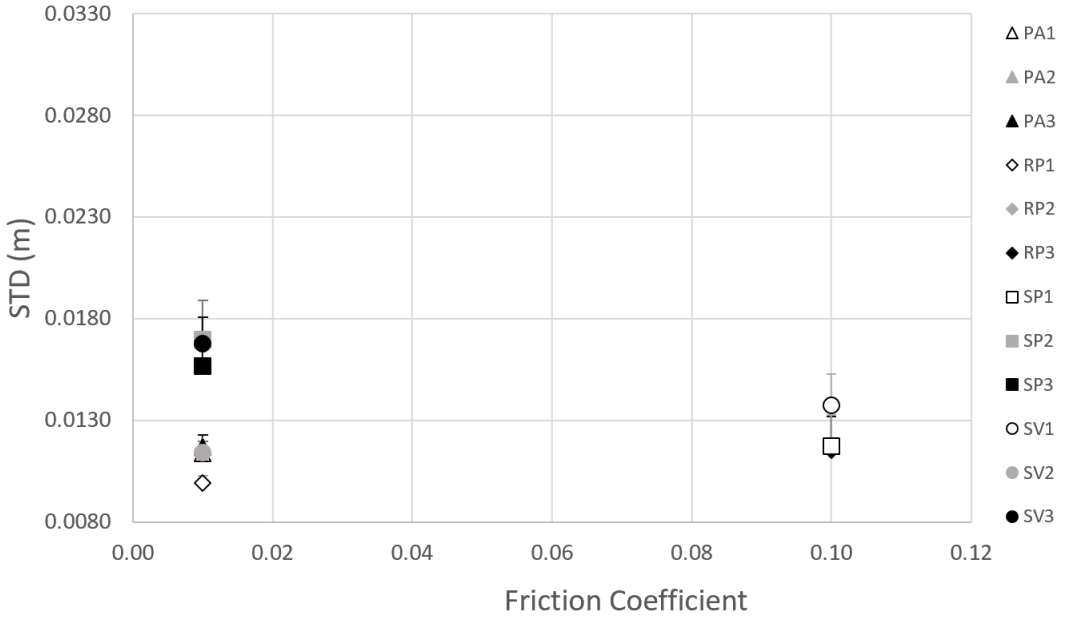

Figure 6.3: The minimum std errors and the corresponding friction coefficients for every vegetated trial. The profile zone is APr.

Next, the rms errors and std values were calculated for the vegetated profile, VPr. The results are shown in Figures 6.4 and 6.5. The minimum values for the respective figures are shown in Tables 6.3 and 6.4.

Table 6.3: The initial rms error values (prior to varying friction coefficients) and the final rms error for VPr.

VPr	PA1	PA2	PA3	RP1	RP2	RP3	SP1	SP2	SP3	SV1	SV2	SV3
Initial (m)	0.0172	0.0184	0.0182	0.0144	0.0218	0.0201	0.0195	0.0276	0.0245	0.0221	0.0135	0.0253
Final (m)	0.0165	0.0183	0.0178	0.0141	0.0173	0.0166	0.0160	0.0249	0.0227	0.0186	0.0125	0.0236
fb	**0.010**	**0.010**	**0.010**	**0.010**	**0.10**	**0.10**	**0.10**	**0.010**	**0.010**	**0.10**	**0.010**	**0.010**

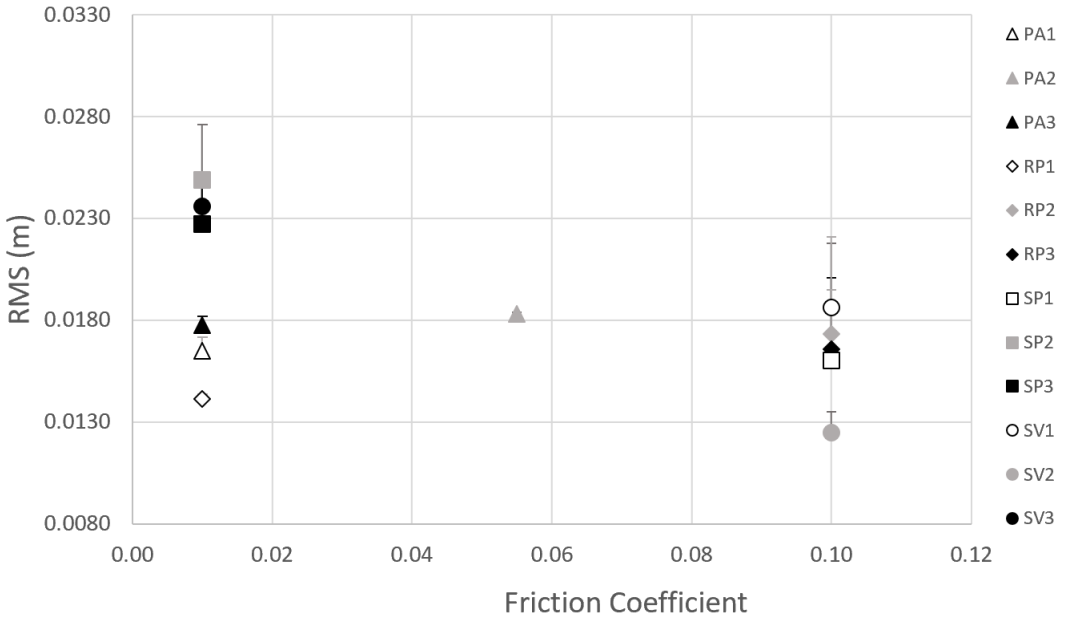

Figure 6.4: The minimum rms errors and the corresponding friction coefficients for every vegetated trial. The profile zone is VPr.

Table 6.4: The initial std error values (prior to varying friction coefficients) and the final std error for VPr.

VPr	PA1	PA2	PA3	RP1	RP2	RP3	SP1	SP2	SP3	SV1	SV2	SV3
Initial (m)	0.0166	0.0175	0.0178	0.0145	0.0205	0.0188	0.0183	0.0277	0.0246	0.0204	0.0133	0.0253
Final (m)	0.0155	0.0172	0.0170	0.0140	0.0164	0.0157	0.0153	0.0250	0.0229	0.0173	0.0125	0.0237
fb	**0.010**	**0.010**	**0.010**	**0.010**	**0.100**	**0.100**	**0.100**	**0.010**	**0.010**	**0.100**	**0.100**	**0.010**

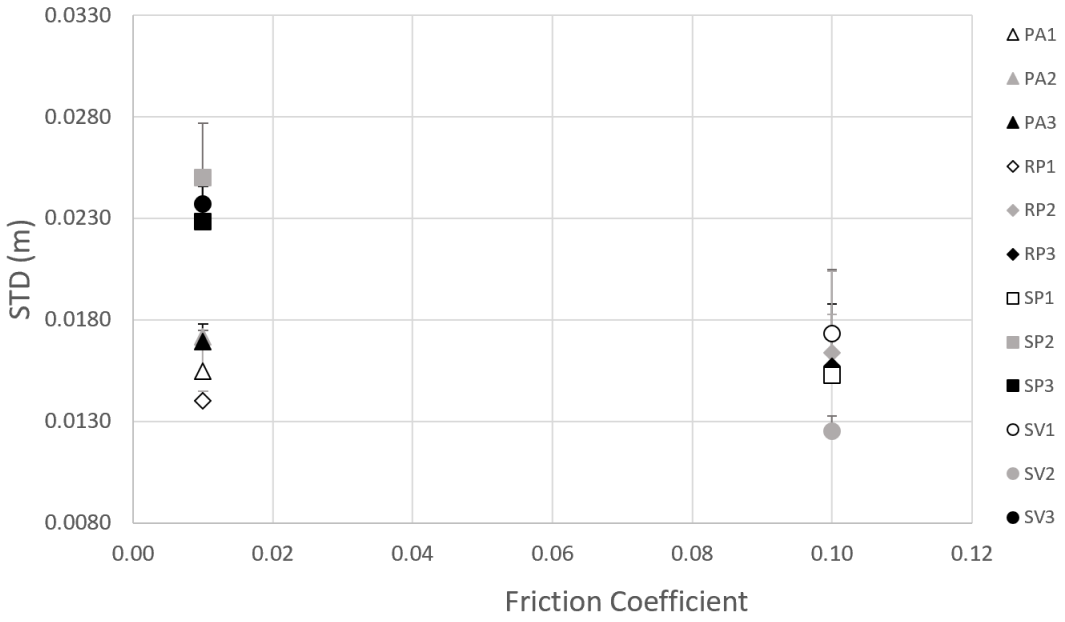

Figure 6.5: The minimum std errors and the corresponding friction coefficients for every vegetated trial. The profile zone is VPr.

Finally, results were also calculated just for the portion of the dune between where scarp retreat begins and where the dune ends, which is defined here as the scarped profile (SPr). The results are shown in Figures 6.6 and 6.7. The corresponding minimum rms and std values and their respective friction coefficients are shown in Tables 6.5 and 6.6.

Table 6.5: The initial rms error values (prior to varying friction coefficients) and the final rms error for SPr.

SPr	PA1	PA2	PA3	RP1	RP2	RP3	SP1	SP2	SP3	SV1	SV2	SV3
Initial (m)	0.0164	0.0166	0.0151	0.0139	0.0228	0.0204	0.0201	0.0293	0.0249	0.0230	0.0116	0.0269
Final (m)	0.0154	0.0166	0.0144	0.0136	0.0169	0.0159	0.0155	0.0256	0.0225	0.0188	0.0109	0.0245
fb	**0.010**	**0.020**	**0.010**	**0.010**	**0.100**	**0.100**	**0.100**	**0.010**	**0.010**	**0.100**	**0.095**	**0.010**

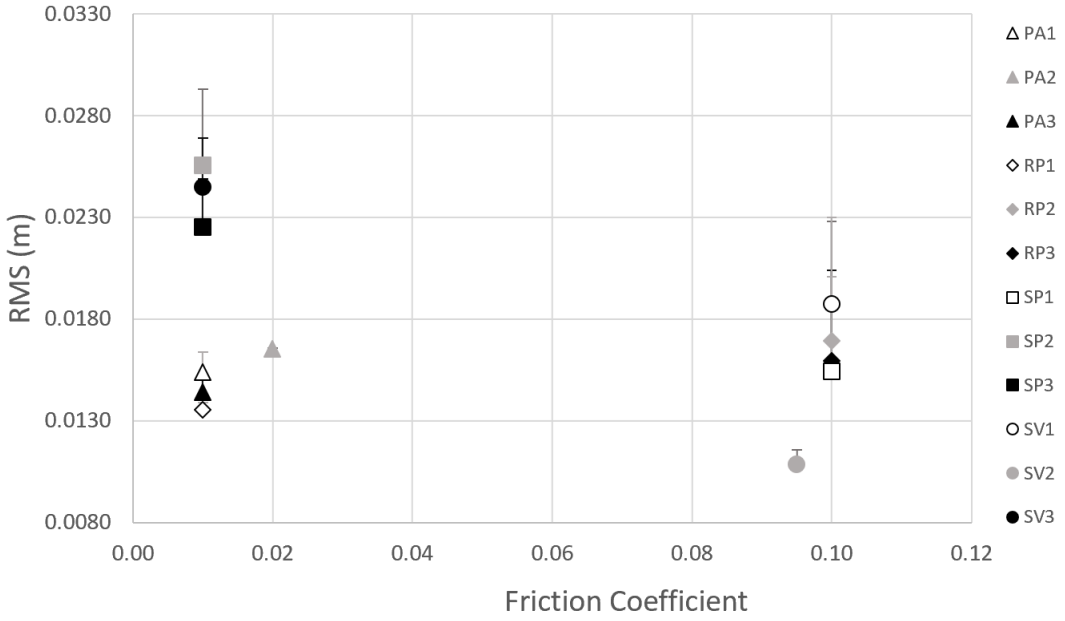

Figure 6.6: The minimum rms errors and the corresponding friction coefficients for every vegetated trial. The profile zone is SPr.

Table 6.6: The initial std error values (prior to varying friction coefficients) and the final std error for SPr.

SPr	PA1	PA2	PA3	RP1	RP2	RP3	SP1	SP2	SP3	SV1	SV2	SV3
Initial (m)	0.0162	0.0165	0.0142	0.0122	0.0229	0.0205	0.0202	0.0245	0.0212	0.0230	0.0109	0.0227
Final (m)	0.0155	0.0165	0.0141	0.0119	0.0171	0.0161	0.0155	0.0213	0.0195	0.0189	0.0092	0.0211
fb	**0.010**	**0.035**	**0.010**	**0.065**	**0.100**	**0.100**	**0.100**	**0.010**	**0.010**	**0.100**	**0.100**	**0.010**

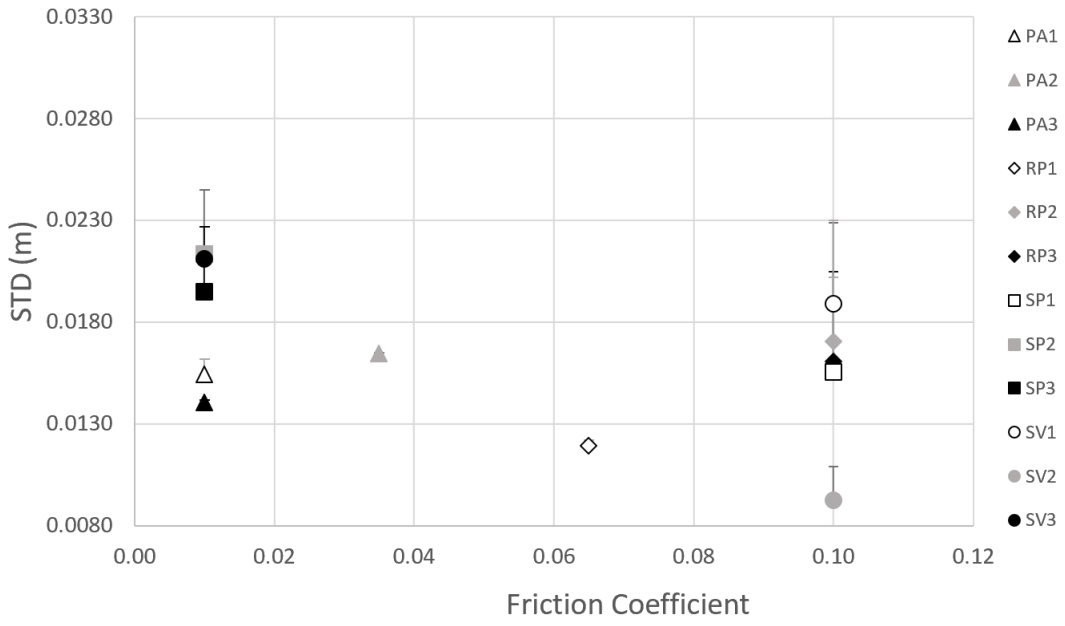

Figure 6.7: The minimum std errors and the corresponding friction coefficients for every vegetated trial. The profile zone is SPr.

6.1.2 Discussion

An important takeaway of this experiment is that the feasibility of representing vegetation within CSHORE as modified friction coefficients within the collision and swash regimes is not as straight forward to simulate as expected. The hypothesis stated that vegetation characteristics (fine root bio-mass, coarse root bio-mass, etc) could be reliably represented as modified friction coefficients, but for most trials this was simply untrue. Notably, only four of the twelve vegetated trials (RP2, RP3, SP1, SV1) showed a negative correlation between the error and an increase in the friction coefficient above the default value ($f_b = 0.02$). This holds true for both rms and std error, which both came out to be nearly identical values, thus indicating that the mean of the difference between the measured and CSHORE results is near zero. The relationship between friction coefficients, vegetation characteristics, and morphological response of the four tests can be assessed by examining the star plots shown previously in Figure 3.4. Interestingly, all four of

the trials have relatively low vegetation characteristics when compared to the trials that indicated a positive correlation between the increasing friction coefficient and error. The only similarity of vegetation characteristics shared by each of the four trials is that they ranked low in all five areas: fine root biomass, coarse root biomass, stem rotational stiffness, above-ground surface area, and mycorrhizal colonization.

Besides the four trials mentioned previously (RP2, RP3, SP1, SV1), the effect of the other trials on the relationship between error and friction coefficients has been examined. Two of three trials (RP1 and SV2) that had a minimal positive correlation between error and friction coefficients both had relatively low vegetation characteristics when compared to all other trials; however, the third trial (PA2) had above average amounts of rotational stiffness, fine root mass, and coarse root mass. In contrast, four of the five trials (PA3, SP2, SP3, and SV3) that showed a relatively large correlation between error and friction coefficients each had a maximum in at least one category, with the only exception being the fifth trial, PA1.

The results indicate that there was no clear indicator of whether or not vegetation characteristics could be represented as varied friction coefficients within CSHORE. This is likely due to the fact that the experiment involves varying the friction coefficients over a short stretch of shoreline (approximately 80 cm) relative to the shape of the waves, which had mean periods of about 1.5 s, peak periods of about 1.8 s, root-mean-square wave heights of approximately 6.5 cm, and wavelengths of approximately 3.4 m. The wavelengths were calculated assuming linear wave theory was applicable at the point of measurement, which had a water depth of 1.03 m. Frictional effects have a stronger influence on wave attenuation over much larger spans, such as in salt flats or salt marshes (Möller, Spencer, French, Leggett, & Dixon, 1999).

6.2 CSHORE-Experiment Similarity by Varying Angle of Repose ϕ

6.2.1 Results

The tangent of the angle of repose ($\tan(\phi)$) was also varied as a means of identifying methods for incorporating vegetation in CSHORE. A default value of 0.63 for sand was chosen, as specified previously. Figure 6.8 shows an example of how the accuracies change with variation of $\tan(\phi)$ for every vegetated trial. In particular, the figure shows the rms error for the active profile.

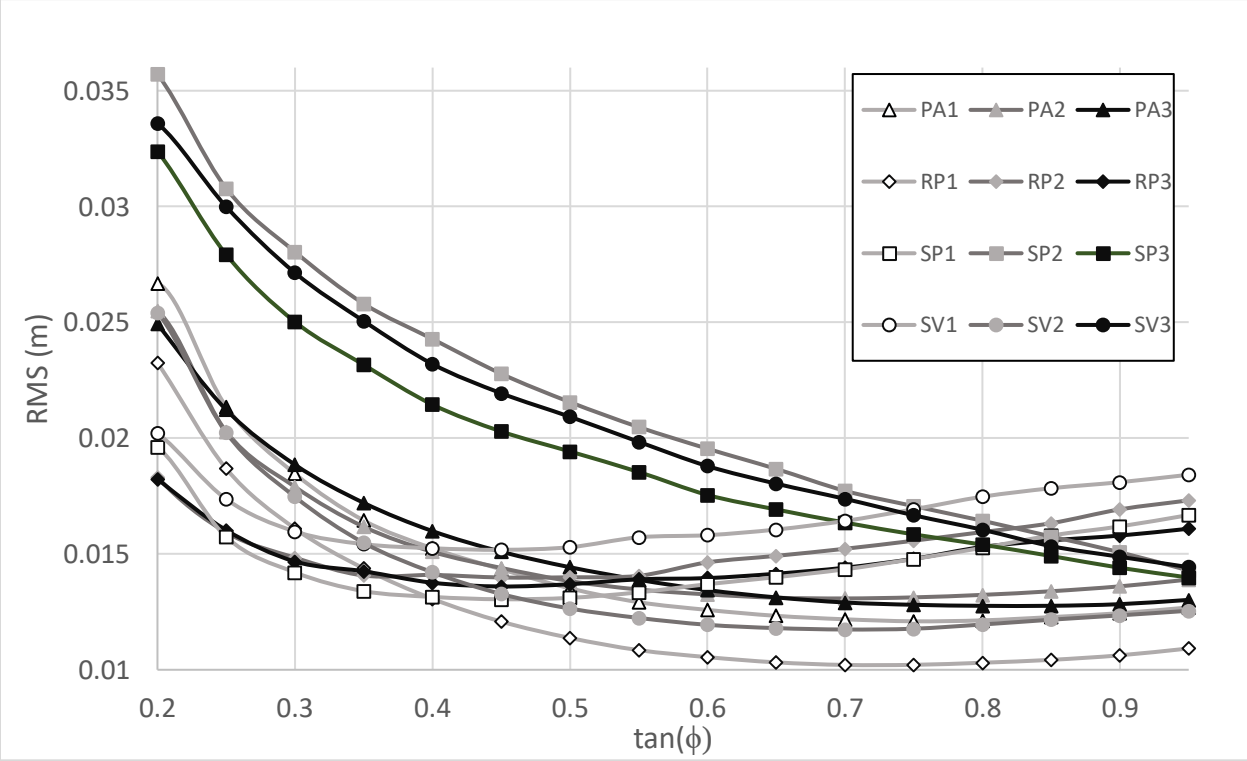

Figure 6.8: Example of change in rms error with variation of $\tan(\phi)$. As can be seen, there exists $\tan(\phi)$ values at which each trial has a minimum rms error.

From the results, $\tan(\phi)$ values corresponding to minimum rms and std errors were found for every trial. The results of this analysis for the active profile are shown in Figures 6.9 (rms) and

6.10 (std). The corresponding initial errors, minimum values, and the corresponding $\tan(\phi)$ at which the minimums occurred are shown in Tables 6.7 and 6.8.

Table 6.7: The initial and minimum rms values and the corresponding $tan(\phi)$ for APr.

APr	PA1	PA2	PA3	RP1	RP2	RP3	SP1	SP2	SP3	SV1	SV2	SV3
Initial (m)	0.0124	0.0131	0.0132	0.0104	0.0148	0.0141	0.0139	0.0190	0.0171	0.0160	0.0119	0.0183
Final (m)	0.0121	0.0131	0.0128	0.0102	0.0140	0.0136	0.0130	0.0143	0.0140	0.0152	0.0117	0.0144
tan(phi)	**0.75**	**0.70**	**0.80**	**0.70**	**0.45**	**0.45**	**0.45**	**0.95**	**0.95**	**0.45**	**0.70**	**0.95**

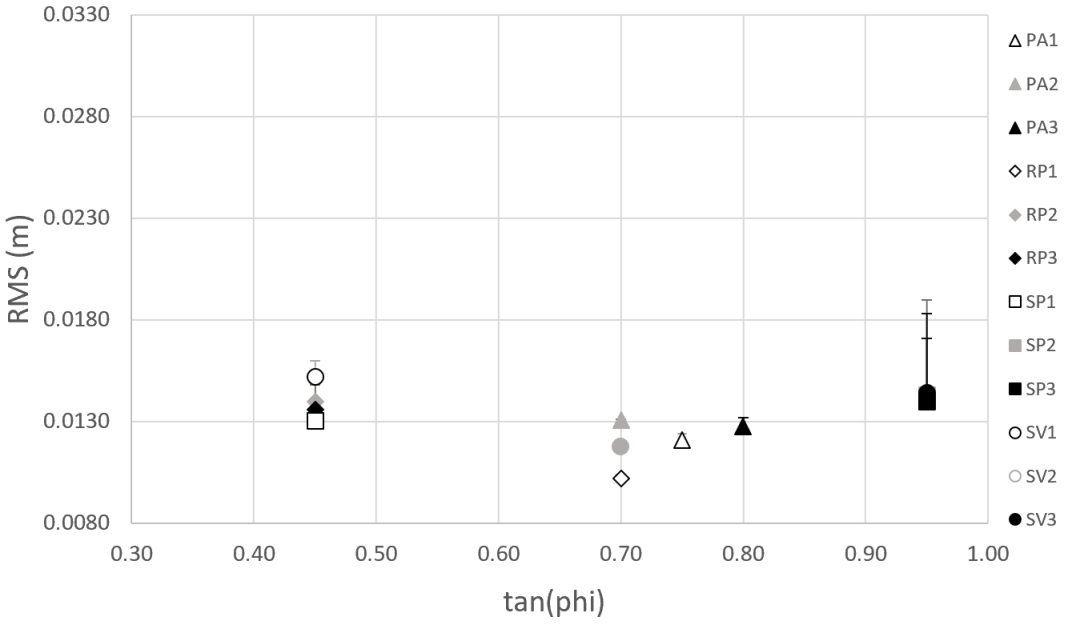

Figure 6.9: The minimum rms errors and the corresponding $tan(\phi)$ values for APr. The error bars indicate the initial errors corresponding to a $tan(\phi)$ value of 0.63.

Table 6.8: The initial and minimum std values and the corresponding $tan(\phi)$ for APr.

APr	PA1	PA2	PA3	RP1	RP2	RP3	SP1	SP2	SP3	SV1	SV2	SV3
Initial (m)	0.0120	0.0120	0.0123	0.0103	0.0141	0.0132	0.0133	0.0189	0.0170	0.0153	0.0117	0.0181
Final (m)	0.0116	0.0118	0.0117	0.0101	0.0133	0.0128	0.0125	0.0140	0.0137	0.0145	0.0116	0.0141
tan(phi)	**0.75**	**0.70**	**0.85**	**0.75**	**0.50**	**0.45**	**0.45**	**0.95**	**0.95**	**0.45**	**0.70**	**0.95**

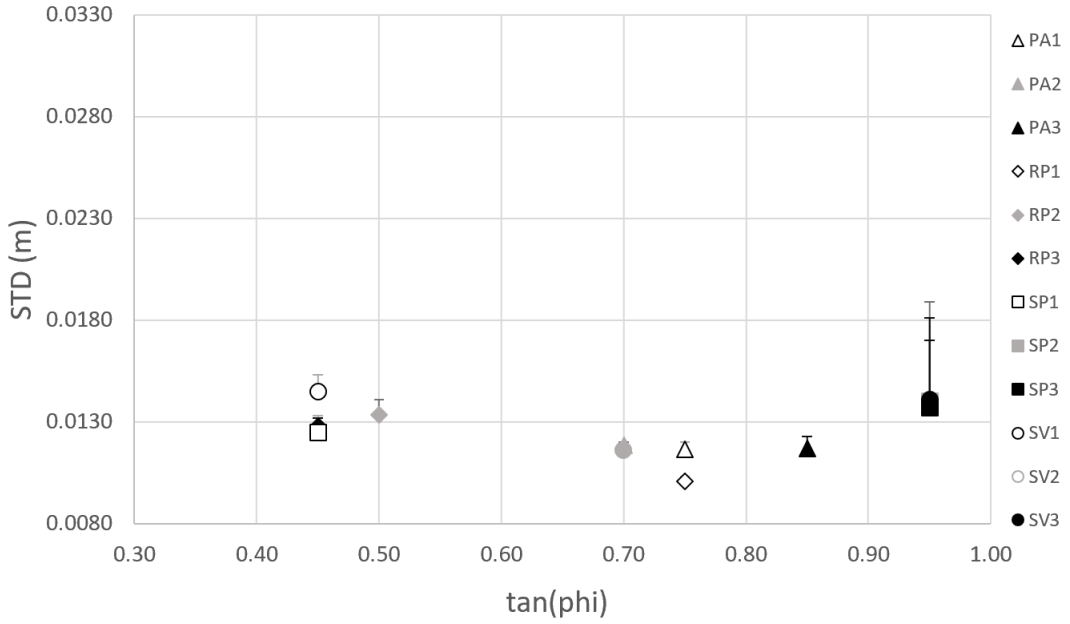

Figure 6.10: The minimum std errors and the corresponding $tan(\phi)$ values for APr.

Moving forward, the variation in rms and std was then calculated for the vegetated profile (VPr). The results are shown for rms and std in Figures 6.11 and 6.12 respectively. The minimum rms and std values and their corresponding $\tan(\phi)$ values are shown in Tables 6.9 and 6.10.

Table 6.9: The initial and minimum rms values and the corresponding $tan(\phi)$ for VPr.

VPr	PA1	PA2	PA3	RP1	RP2	RP3	SP1	SP2	SP3	SV1	SV2	SV3
Initial (m)	0.0172	0.0184	0.0182	0.0144	0.0218	0.0201	0.0195	0.0276	0.0245	0.0221	0.0135	0.0253
Final (m)	0.0166	0.0184	0.0177	0.0140	0.0198	0.0190	0.0179	0.0203	0.0193	0.0197	0.0134	0.0198
tan(phi)	0.75	0.65	0.75	0.75	0.35	0.45	0.45	0.95	0.95	0.35	0.65	0.95

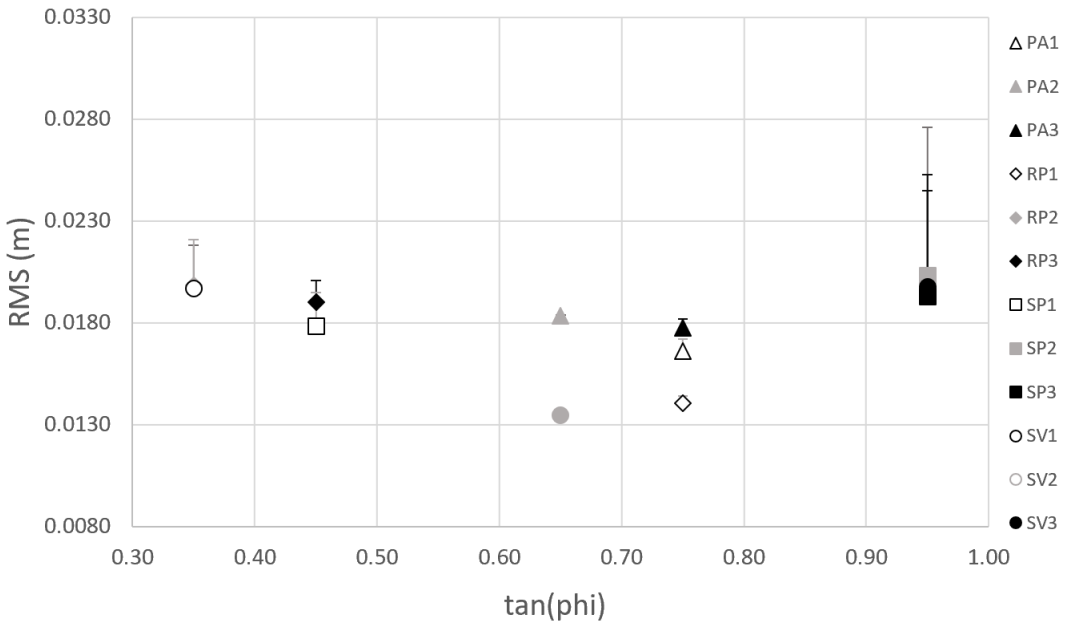

Figure 6.11: The minimum rms errors and the corresponding $tan(\phi)$ values for VPr.

Table 6.10: The initial and minimum std values and the corresponding $tan(\phi)$ for VPr.

VPr	PA1	PA2	PA3	RP1	RP2	RP3	SP1	SP2	SP3	SV1	SV2	SV3
Initial (m)	0.0172	0.0184	0.0182	0.0144	0.0218	0.0201	0.0195	0.0276	0.0245	0.0221	0.0135	0.0253
Final (m)	0.0143	0.0168	0.0159	0.0136	0.0197	0.0188	0.0177	0.0203	0.0190	0.0198	0.0127	0.0197
tan(phi)	**0.95**	**0.85**	**0.90**	**0.85**	**0.55**	**0.65**	**0.50**	**0.95**	**0.95**	**0.45**	**0.75**	**0.95**

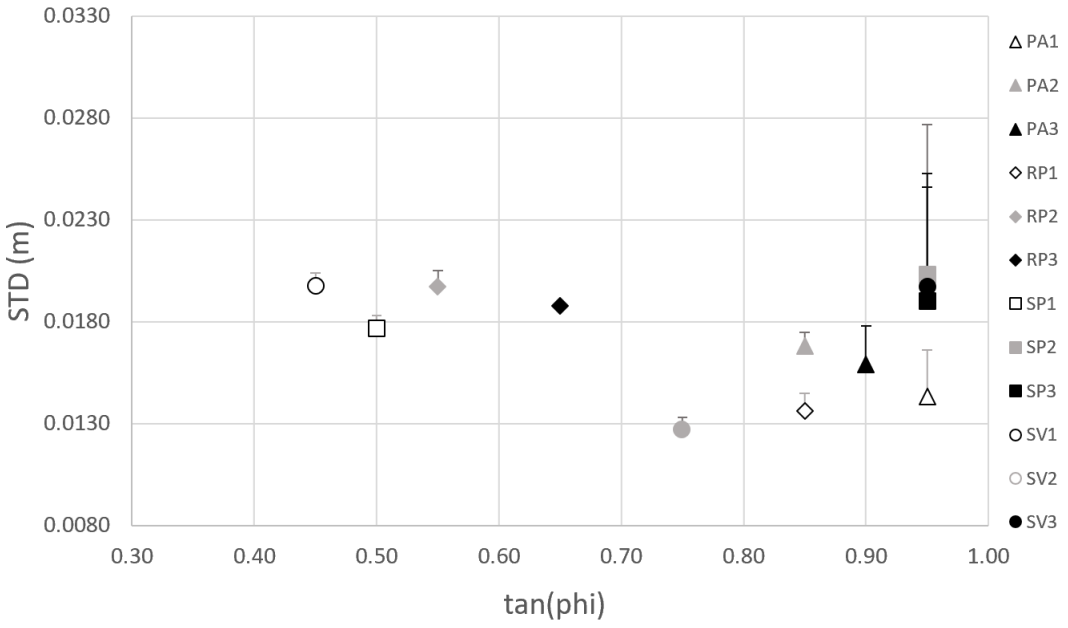

Figure 6.12: The minimum std errors and the corresponding $tan(\phi)$ values for VPr.

Finally, the accuracy was assessed strictly in the zone of dune scarp retreat, SPr. The rms and std errors of these tests are shown in Figures 6.13 and 6.14 respectively. The corresponding minimum rms and std values and their $\tan(\phi)$ counterparts are shown in Tables 6.11 and 6.12.

Table 6.11: The initial and minimum rms values and the corresponding $tan(\phi)$ for SPr.

SPr	PA1	PA2	PA3	RP1	RP2	RP3	SP1	SP2	SP3	SV1	SV2	SV3
Initial (m)	0.0164	0.0166	0.0151	0.0139	0.0228	0.0204	0.0201	0.0293	0.0249	0.023	0.0116	0.0269
Final (m)	0.0154	0.0165	0.0141	0.0133	0.0206	0.0192	0.0181	0.0188	0.0172	0.0205	0.0114	0.0189
tan(phi)	**0.80**	**0.65**	**0.80**	**0.75**	**0.35**	**0.45**	**0.45**	**0.95**	**0.95**	**0.40**	**0.70**	**0.95**

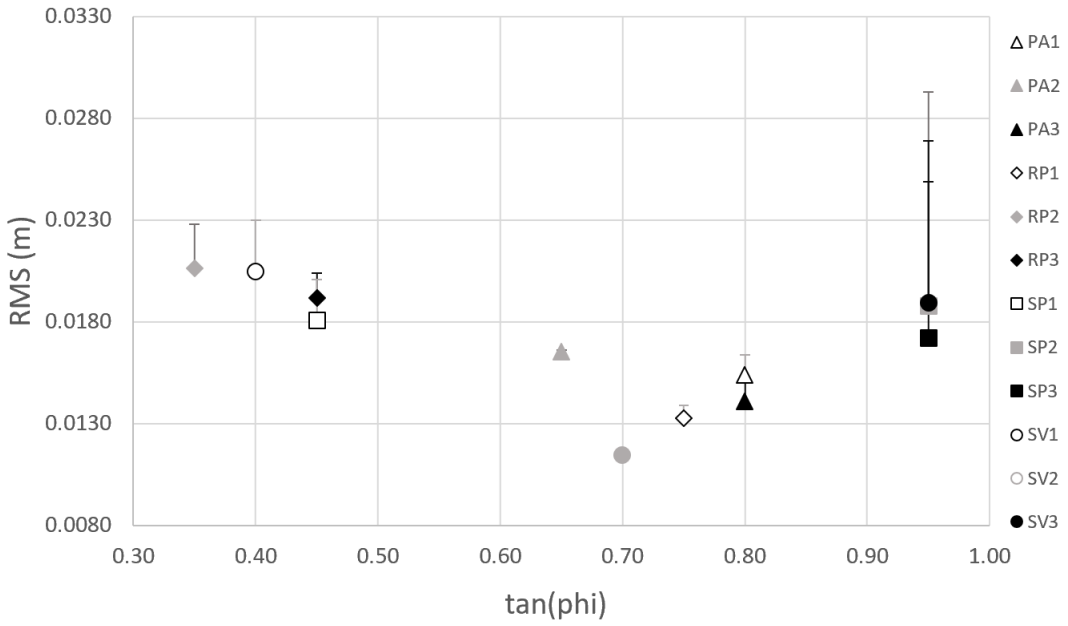

Figure 6.13: The minimum rms errors and the corresponding $tan(\phi)$ values for SPr.

Table 6.12: The initial and minimum std values and the corresponding $tan(\phi)$ for SPr.

SPr	PA1	PA2	PA3	RP1	RP2	RP3	SP1	SP2	SP3	SV1	SV2	SV3
Initial (m)	0.0162	0.0165	0.0142	0.0122	0.0229	0.0205	0.0202	0.0245	0.0212	0.023	0.0109	0.0227
Final (m)	0.0155	0.0165	0.0140	0.0122	0.0180	0.0182	0.0159	0.0167	0.0161	0.0172	0.0107	0.0176
tan(phi)	**0.80**	**0.60**	**0.70**	**0.60**	**0.20**	**0.30**	**0.30**	**0.95**	**0.95**	**0.25**	**0.55**	**0.95**

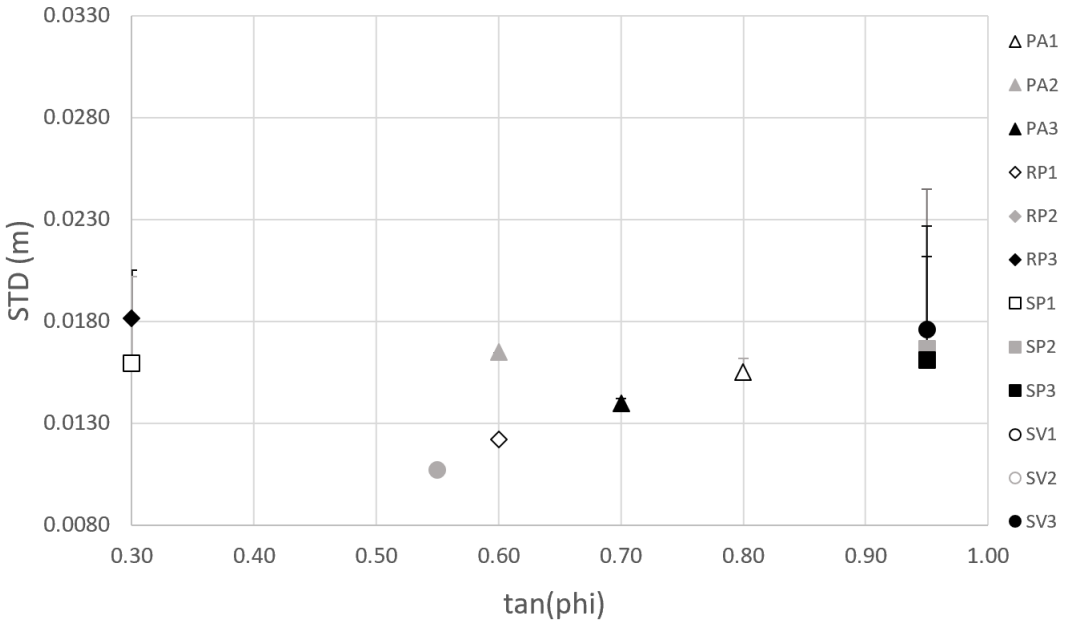

Figure 6.14: The minimum std errors and the corresponding $tan(\phi)$ values for SPr.

6.2.2 Discussion

Unlike the friction coefficients which can be varied at any cross-shore location, the tangent of the angle of repose of sediment is applied to the entire profile. This is not expected to be a problem since the impact on the profile will only occur at the scarp due to the effect of the scarping/slumping routine within CSHORE. This contrasts with the application of the bed friction coefficients, which can be varied at any cross-shore location along the profile. The trials that showed a negative correlation between error and $\tan(\phi)$ for each of the zones considered (APr, VPr, and SPr) are shown in Table 6.13.

Table 6.13: Trials showing a negative correlation between error and increase in $tan(\phi)$ from the default value of $tan(\phi) = 0.63$.

	Active Profile	**Vegetated Profile**	**Scarped Profile**
Rms	PA1, PA2, PA3, RP1, SP2, SP3, SV2, SV3	PA1, PA2, PA3, RP1, SP2, SP3, SV2, SV3	PA1, PA2, PA3, RP1, SP2, SP3, SV2, SV3
Std	PA1, PA2, PA3, RP1, SP2, SP3, SV2, SV3	PA1, PA2, PA3, RP1, RP3, SP2, SP3, SV2, SV3	PA1, PA3, SP2, SP3, SV3

Interestingly, eight of the twelve trials showed that an increase in the angle of repose of the entire shoreline produced a more accurate comparison between the experimental and CSHORE profiles, with only four trials excluded (RP2, RP3, SP1, SV1). For the trials that showed a stronger negative correlation between error and $\tan(\phi)$, the most defining feature is coarse root mass. The rotational stiffness, fine root mass, and surface area were all of relatively high importance compared to that of the excluded trials. The only feature that bore no apparent role was the mycorrhizal population.

All of the excluded trials feature some of the lowest vegetation characteristics with each having every single vegetation parameter below average. Notably, the mycorrhizal population was also very low for these trials. Since mycorrhizal fungi population was very low throughout all trials, it can be assumed that it had no practical effect on error vs $\tan(\phi)$ relationship. This is likely due to the fact that young vegetation was used, so the fungi population did not have enough time to develop.

The influence of the vegetation on scarp steepness can be seen in Figure 6.15, where the optimized profile elevations of SP2, SP3, and SV3 (the trials that experienced the highest increase in accuracy after $\tan(\phi)$ variation) are compared against the elevations corresponding to the

default $\tan(\phi)$ value of 0.63. For each of these trials, the optimal $\tan(\phi)$ value was 0.95. The figure provides insight into the influence of the variation of the tangent of the angle of repose on the accuracy of CSHORE. Within each subfigure, it can be seen that increasing $\tan(\phi)$ caused more sediment to remain on the dune, which is due to the fact that the bottom slope function within CSHORE instigates offshore bedload only when the scarp has become steeper than the angle of repose to simulate scarp retreat.

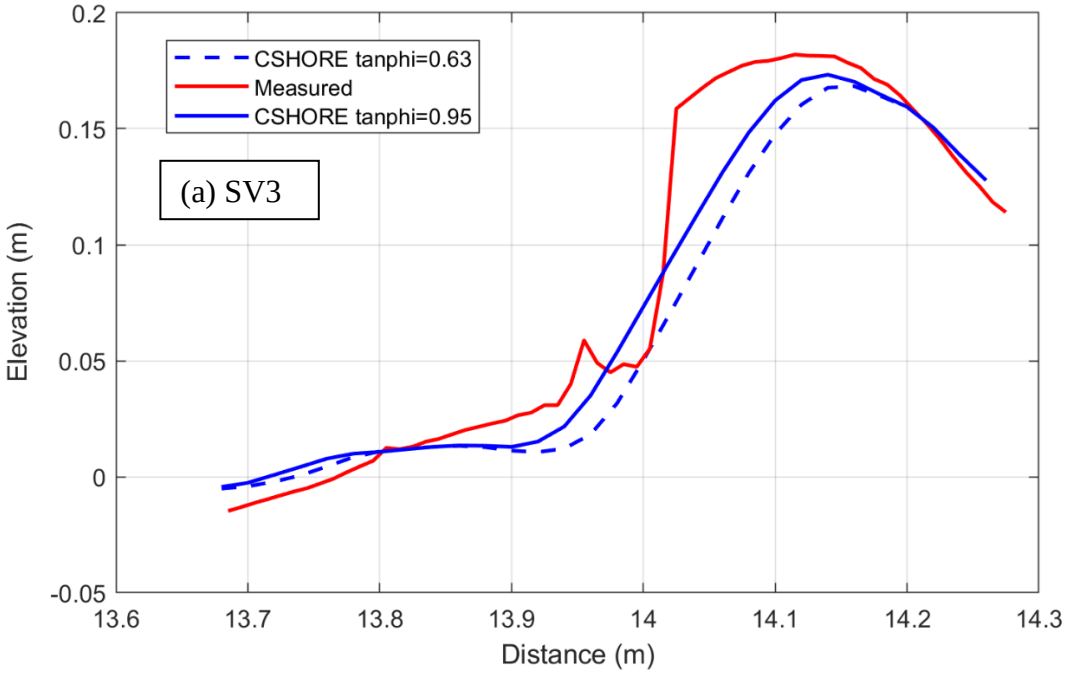
CSHORE tanphi=0.63
Measured
CSHORE tanphi=0.95
(a) SV3
Elevation (m)
Distance (m)
0.2
0.15
0.1
0.05
0
-0.05
13.6
13.7
13.8
13.9
14
14.1
14.2
14.3

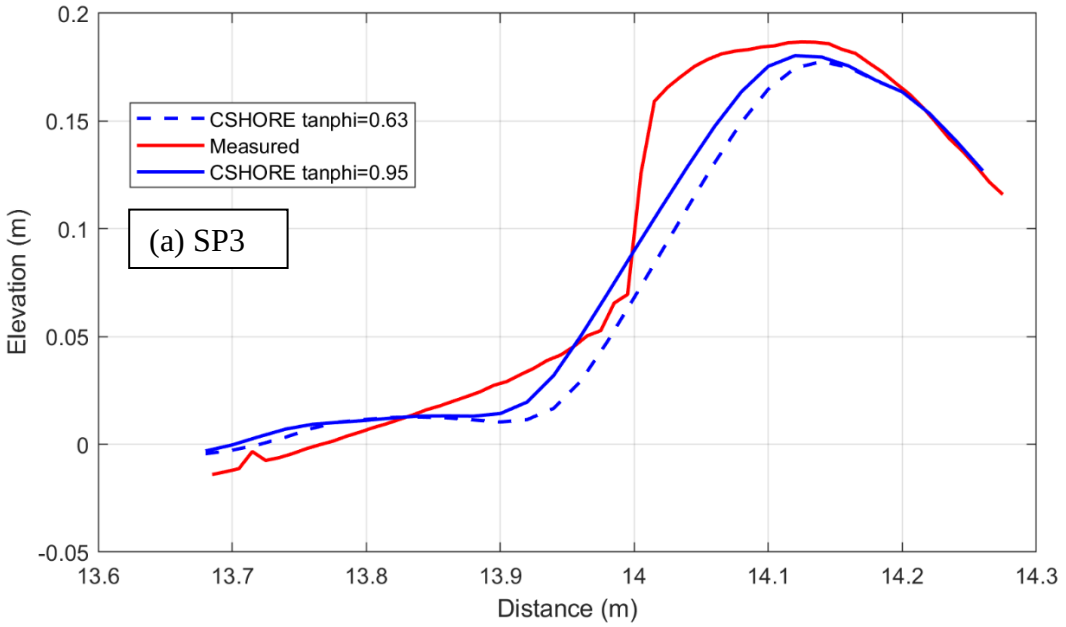
CSHORE tanphi=0.63
Measured
CSHORE tanphi=0.95
(a) SP3
Elevation (m)
Distance (m)
0.2
0.15
0.1
0.05
0
-0.05
13.6
13.7
13.8
13.9
14
14.1
14.2
14.3

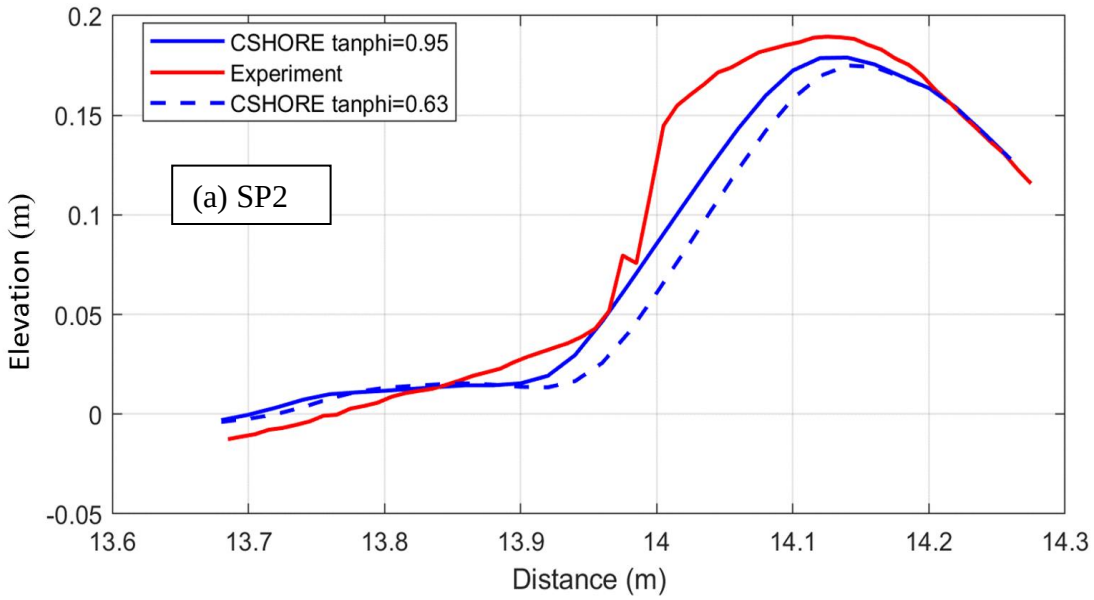

Figure 6.15: Final profiles of the measured experimental profile (red) and the CSHORE output (blue) for the SPr zone. (a) Shows trial SV3, (b) shows trial SP2, and (c) shows trial SP3. This figure demonstrates how CSHORE conformed to the measured results after an optimal $tan(\phi)$ *was found.*

6.3 General Comments on CSHORE Accuracy

The relatively low rms and std error of the profile difference between the experimental and CSHORE results indicate that CSHORE performed as expected based on case studies. The difference between the initial CSHORE and experimental results could lie in the fact that CSHORE moves material downslope whenever sediment transport formulations cause the angle of the profile to become too steep to account for the angle of repose.

The similarity of profile evolutions calculated by CSHORE to profile evolutions from the control trials is satisfactorily accurate when compared to similar experiments involving CSHORE case studies (Kobayashi, 2013). The main difference between the two is apparent by a larger deposition of sand immediately in front of the dune within the CSHORE results. This involves CSHORE's tendency to move sediment downslope when the angle of the shoreline is too steep. The results of the case studies indicated an rms error of approximately 0.6 m for a cross-shore

profile ranging 14 meters in height. For the performed experiments, the rms error for trial C1 and C2 were 1.5 cm and 1.75 cm respectively for a profile elevation spanning 33 cm. The ratio of profile elevation to rms error is 0.045 and 0.053 for the two control trials and 0.043 for the case study, indicating that CSHORE is performing as it should for the present work.

CHAPTER VII

CONCLUSIONS AND FUTURE WORK

This thesis was based on work performed by Dr. Jake Sigren for his dissertation, in which he related morphological changes in sand dune profiles and hydrodynamic changes in the swash zone to the presence of vegetation on the dune and within the swash. His findings indicated that above-ground surface area resulted in lower turbulent kinetic energy within the swash zone, and that a combination of above and below-ground characteristics resulted in a reduction of erosion and an increased steepness of dune scarping. The present work explored how these results may be reflected in CSHORE, the results of which provide insight into which parameters to consider when modeling vegetation within CSHORE. These results may also have implications within other numerical, process-based, cross-shore evolution models such as XBEACH and SBEACH.

The key findings from this experiment indicate that representing vegetation as friction coefficients within CSHORE is not a viable approach when modeling sediment transport. The friction coefficients ranged in value from 0.01 to 0.1 with 0.02 being the default value commonly chosen for sandy beaches. Most vegetation was best represented by friction coefficients of either 0.01 or 0.1, but there was no clear relation between increased accuracy due to friction coefficient variation and specific vegetation characteristics, regardless of whether those characteristics were above ground (surface area, stem rotational stiffness) or below ground (root mass, mycorrhizal colonization). A probable reason for this is that friction coefficients are more influential when the measured area is much larger than the one used for this experiment.

In addition to varying friction coefficients, the dune vegetation was separately represented in the numerical model as increasing tangents of the angle of repose ($\tan(\phi)$), which were varied in value from 0.05 to 0.95 with a default value of 0.63, which is generally accepted within the literature as the default value for sandy beaches. From this analysis, it was found that as the angle of repose increased, most of the results became more accurate, thus indicating that the vegetation could be represented as an increasing angle of repose. Interestingly, vegetation with larger amounts of above-ground and below-ground characteristics produced more accurate results, and the most accurate results occurred at much higher tangents of the angle of repose. This indicates that the angle of repose is an important characteristic to consider when modeling vegetation within CSHORE. The sample size was not large enough to give a quantitative recommendation for which $\tan(\phi)$ to use when modeling vegetation in CSHORE. However, for the data that is available, it was shown that dense vegetation was consistently represented best by $\tan(\phi) = 0.95$.

The relationship between the vegetation and the angle of repose should be studied more in depth. The angle of repose can only be set for the entire shoreline within CSHORE. Since the angle of repose may represent vegetation better than other parameters, it is probable that even more accurate results could be obtained by incorporating a subroutine into CSHORE to allow for the variation of the angle of repose strictly within the vegetated section of the profile. Alternatively, this may not be important since the steepest shoreline slopes occur only where scarping is present, thus alteration of offshore features such as sand bars and runnels by changing the angle of repose is unlikely.

Variation of the bed friction coefficients poorly simulated the effect of vegetation on morphodynamics, but its effect on hydrodynamics should be studied further. Friction coefficients are better known for influencing hydrodynamics than they are for altering shoreline elevations

over short distances, and more experiments would be able to confirm this observation. More experiments should be conducted to assess the influence of varied friction coefficients and $\tan(\phi)$ values on the hydrodynamics and profile evolution of other numerical models, such as SBEACH and XBEACH.

Finally, more physical experiments with more types of vegetation should be performed in order to increase the sample size of data regarding the influence of vegetation on dune morphodynamics and nearshore hydrodynamics.

REFERENCES

Bailard, J. A. (1981). An energetics total load sediment transport model for a plane sloping beach. *Journal of Geophysical Research: Oceans, 86*(C11), 10938-10954.

Bryant, D. B., Bryant, M. A., & Grzegorzewski, A. S. (2017). *Erosion of Coastal Foredunes: A Review on the Effect of Dune Vegetation*. Retrieved from

Cowles, H. C. (1899). The Ecological Relations of the Vegetation on the Sand Dunes of Lake Michigan. Part I.-Geographical Relations of the Dune Floras. *Botanical gazette, 27*(2), 95-117.

Dalrymple, R. A., & Kirby, J. T. (1988). Models for very wide-angle water waves and wave diffraction. *Journal of Fluid Mechanics, 192*, 33-50.

Feagin, R. A., Figlus, J., Zinnert, J. C., Sigren, J., Martínez, M. L., Silva, R., . . . Carter, G. (2015). Going with the flow or against the grain? The promise of vegetation for protecting beaches, dunes, and barrier islands from erosion. *Frontiers in Ecology and the Environment, 13*(4), 203-210.

Figlus, J., Sigren, J. M., Power, M. J., & Armitage, R. (2017). *Physical model experiment investigating interactions between different dune vegetation and morphology changes under wave impact*. Paper presented at the Proceedings of Coastal Dynamics.

Fosberg, F. R., & Chapman, V. (1971). Mangroves v. Tidal Waves. *Biological Conservation, 4*(1), 38-39.

Hasselmann, K., Barnett, T., Bouws, E., Carlson, H., Cartwright, D., Enke, K., . . . Kruseman, P. (1973). Measurements of wind-wave growth and swell decay during the Joint North Sea Wave Project (JONSWAP). *Ergänzungsheft*, 8-12.

Kobayashi, N. (2013). Cross-shore numerical model CSHORE 2013 for sand beaches and coastal structures. *Research Rep. No. CACR-13, 1*.

Kobayashi, N., Gralher, C., & Do, K. (2013). Effects of woody plants on dune erosion and overwash. *Journal of Waterway, Port, Coastal, Ocean Engineering, 139*(6), 466-472.

Larson, M., Kraus, N. C., & Byrnes, M. R. (1990). *Sbeach: Numerical model for simulating storm-induced beach change. report 2. numerical formulation and model tests*. Retrieved from

McGranahan, G., Balk, D., & Anderson, B. (2007). The rising tide: assessing the risks of climate change and human settlements in low elevation coastal zones. *Environment Urbanization, 19*(1), 17-37.

Möller, I., Spencer, T., French, J. R., Leggett, D., & Dixon, M. (1999). Wave transformation over salt marshes: a field and numerical modelling study from North Norfolk, England. *Estuarine, Coastal and Shelf Science, 49*(3), 411-426.

National Beach Nourishment Database. (2019). Retrieved from https://coast.noaa.gov/digitalcoast/tools/beach-nourishment.html

Phillips, O. M. (1977). The Dynamics of the Upper Ocean.

Pietropaolo, J., Kobayashi, N., & Melby, J. A. (2012). Wave runup on dikes and beaches. *Coastal Engineering, 1*(33), 19.

Roelvink, D., Reniers, A., Van Dongeren, A., de Vries, J. v. T., McCall, R., & Lescinski, J. (2009). Modelling storm impacts on beaches, dunes and barrier islands. *Coastal Engineering, 56*(11-12), 1133-1152.

Roelvink, J. A., & Brøker, I. (1993). Cross-shore profile models. *Coastal Engineering, 21*(1-3), 163-191.

Ruiz, G. (2007). Sediment Transport Outside the Surf Zone Model. Retrieved from www.mathworks.com/matlabcentral/fileexchange

Sigren, J. M. (2017). *Coastal Dunes and Dune Vegetation: Interdisciplinary Research on Storm Protection, Erosion, and Ecosystem Restoration.*

Silva, R., Martínez, M., Odériz, I., Mendoza, E., & Feagin, R. (2016). Response of vegetated dune–beach systems to storm conditions. *Coastal Engineering, 109,* 53-62.

Stallins, J. A., & Parker, A. J. (2003). The influence of complex systems interactions on barrier island dune vegetation pattern and process. *Annals of the Association of American Geographers, 93*(1), 13-29.

Strelzoff, A. (2019). About EWN. Retrieved from https://ewn.el.erdc.dren.mil/about.html#_

APPENDIX

```
3                                   -> NLINES
------------------------------------------------------------
Test PA1, SWL=0.0m, Planar slope erosion
------------------------------------------------------------
1                                   -> IPROFL
1                                   -> ISEDAV
0                                   -> IPERM
1                                   -> IOVER
0                                   -> IWTRAN
0                                   -> IPOND
0                                   -> INFILT
0                                   -> IWCINT
1                                   -> IROLL
0                                   -> IWIND
0                                   -> ITIDE
0.02                                -> DX
0.6000                              -> GAMMA
0.1520    0.0110    2.6500          -> D50,WF,SG
0.0038    0.0060    0.1800    0.3000    -> EFFB,EFFF,SLP,SLPOT
0.95      0.0050                    -> TANPHI,BLP
0.0200                              -> RWH
1       -> ILAB
12      -> NWAVE
12      -> NSURGE
209.95    1.8696    0.065282  0       0       0
419.9     1.8696    0.064167  0       0       0
629.85    1.8696    0.064122  0       0       0
839.8     1.8696    0.064041  0       0       0
1049.75   1.8696    0.06388   0       0       0
1259.7    1.8696    0.063486  0       0       0
1469.65   1.8696    0.064469  0       0       0
1679.6    1.8696    0.063943  0       0       0
1889.55   1.8696    0.061756  0       0       0
2099.5    1.8696    0.062271  0       0       0
2309.45   1.9422    0.062448  0       0       0
2519.4    1.9422    0.061953  0       0       0
```

710 -> NBINP

7 -> NPINP

0 -0.912 0.02

1.1766 -0.912 0.02

1.595 -0.809 0.02

3.35 -0.377 0.02

7.225 -0.30651 0.02

7.235 -0.30651 0.02

7.245 -0.30587 0.02

7.255 -0.30687 0.02

7.265 -0.30707 0.02

7.275 -0.30662 0.02

7.285 -0.30653 0.02

7.295 -0.30623 0.02

7.305 -0.30595 0.02

7.315 -0.30487 0.02

7.325 -0.30458 0.02

7.335 -0.30469 0.02

7.345 -0.30529 0.02

7.355 -0.30548 0.02

7.365 -0.30524 0.02

7.375 -0.30385 0.02

7.385 -0.30317 0.02

7.395 -0.30439 0.02

7.405 -0.30534 0.02

7.415 -0.30536 0.02

7.425 -0.30511 0.02

7.435 -0.30505 0.02

7.445 -0.30557 0.02

7.455 -0.30485 0.02

7.465 -0.30498 0.02

7.475 -0.30593 0.02

7.485 -0.30505 0.02

7.495 -0.30362 0.02

7.505 -0.30381 0.02

7.515 -0.30433 0.02

7.525 -0.30434 0.02

7.535 -0.3025 0.02

7.545 -0.30067 0.02

7.555 -0.30035 0.02

7.565	-0.30047	0.02
7.575	-0.30038	0.02
7.585	-0.30009	0.02
7.595	-0.29811	0.02
7.605	-0.29651	0.02
7.615	-0.29616	0.02
7.625	-0.29704	0.02
7.635	-0.29846	0.02
7.645	-0.29854	0.02
7.655	-0.29805	0.02
7.665	-0.2973	0.02
7.675	-0.29603	0.02
7.685	-0.29579	0.02
7.695	-0.29614	0.02
7.705	-0.29606	0.02
7.715	-0.29494	0.02
7.725	-0.29443	0.02
7.735	-0.29411	0.02
7.745	-0.29347	0.02
7.755	-0.29352	0.02
7.765	-0.29497	0.02
7.775	-0.29584	0.02
7.785	-0.29629	0.02
7.795	-0.29527	0.02
7.805	-0.29453	0.02
7.815	-0.29465	0.02
7.825	-0.2956	0.02
7.835	-0.29596	0.02
7.845	-0.29412	0.02
7.855	-0.29249	0.02
7.865	-0.29363	0.02
7.875	-0.29295	0.02
7.885	-0.29345	0.02
7.895	-0.29499	0.02
7.905	-0.29479	0.02
7.915	-0.29346	0.02
7.925	-0.29391	0.02
7.935	-0.29365	0.02
7.945	-0.29254	0.02
7.955	-0.29395	0.02

7.965	-0.29528	0.02
7.975	-0.29508	0.02
7.985	-0.29371	0.02
7.995	-0.2923	0.02
8.005	-0.29264	0.02
8.015	-0.29244	0.02
8.025	-0.29218	0.02
8.035	-0.29181	0.02
8.045	-0.29062	0.02
8.055	-0.29091	0.02
8.065	-0.29176	0.02
8.075	-0.29196	0.02
8.085	-0.29189	0.02
8.095	-0.29241	0.02
8.105	-0.29208	0.02
8.115	-0.29137	0.02
8.125	-0.29065	0.02
8.135	-0.29007	0.02
8.145	-0.28984	0.02
8.155	-0.2912	0.02
8.165	-0.29276	0.02
8.175	-0.2916	0.02
8.185	-0.28969	0.02
8.195	-0.28827	0.02
8.205	-0.28717	0.02
8.215	-0.28601	0.02
8.225	-0.28573	0.02
8.235	-0.28663	0.02
8.245	-0.28866	0.02
8.255	-0.28812	0.02
8.265	-0.28774	0.02
8.275	-0.28689	0.02
8.285	-0.28618	0.02
8.295	-0.28611	0.02
8.305	-0.28704	0.02
8.315	-0.28795	0.02
8.325	-0.28938	0.02
8.335	-0.28812	0.02
8.345	-0.28746	0.02
8.355	-0.28718	0.02

8.365 -0.28531 0.02

8.375 -0.2843 0.02

8.385 -0.28268 0.02

8.395 -0.28154 0.02

8.405 -0.2807 0.02

8.415 -0.28091 0.02

8.425 -0.28154 0.02

8.435 -0.28334 0.02

8.445 -0.2836 0.02

8.455 -0.282 0.02

8.465 -0.28087 0.02

8.475 -0.28116 0.02

8.485 -0.28117 0.02

8.495 -0.27996 0.02

8.505 -0.28066 0.02

8.515 -0.28316 0.02

8.525 -0.28455 0.02

8.535 -0.28293 0.02

8.545 -0.28183 0.02

8.555 -0.28166 0.02

8.565 -0.28144 0.02

8.575 -0.2808 0.02

8.585 -0.27977 0.02

8.595 -0.28113 0.02

8.605 -0.28083 0.02

8.615 -0.2808 0.02

8.625 -0.27931 0.02

8.635 -0.27839 0.02

8.645 -0.27795 0.02

8.655 -0.27782 0.02

8.665 -0.27852 0.02

8.675 -0.27824 0.02

8.685 -0.27953 0.02

8.695 -0.28056 0.02

8.705 -0.28162 0.02

8.715 -0.28162 0.02

8.725 -0.2814 0.02

8.735 -0.27963 0.02

8.745 -0.27851 0.02

8.755 -0.28046 0.02

8.765	-0.28104	0.02
8.775	-0.28001	0.02
8.785	-0.2779	0.02
8.795	-0.27745	0.02
8.805	-0.27848	0.02
8.815	-0.27894	0.02
8.825	-0.2801	0.02
8.835	-0.27992	0.02
8.845	-0.27866	0.02
8.855	-0.27666	0.02
8.865	-0.27626	0.02
8.875	-0.2761	0.02
8.885	-0.27585	0.02
8.895	-0.27606	0.02
8.905	-0.27603	0.02
8.915	-0.2769	0.02
8.925	-0.2745	0.02
8.935	-0.27243	0.02
8.945	-0.27129	0.02
8.955	-0.27001	0.02
8.965	-0.27001	0.02
8.975	-0.27169	0.02
8.985	-0.27202	0.02
8.995	-0.27154	0.02
9.005	-0.2716	0.02
9.015	-0.27175	0.02
9.025	-0.27285	0.02
9.035	-0.27346	0.02
9.045	-0.27396	0.02
9.055	-0.27363	0.02
9.065	-0.27345	0.02
9.075	-0.27307	0.02
9.085	-0.27305	0.02
9.095	-0.27247	0.02
9.105	-0.27275	0.02
9.115	-0.27249	0.02
9.125	-0.27145	0.02
9.135	-0.26998	0.02
9.145	-0.26956	0.02
9.155	-0.2691	0.02

9.165	-0.26676	0.02
9.175	-0.26704	0.02
9.185	-0.26847	0.02
9.195	-0.2682	0.02
9.205	-0.26775	0.02
9.215	-0.26752	0.02
9.225	-0.26697	0.02
9.235	-0.26709	0.02
9.245	-0.26701	0.02
9.255	-0.26689	0.02
9.265	-0.26697	0.02
9.275	-0.26658	0.02
9.285	-0.2665	0.02
9.295	-0.26648	0.02
9.305	-0.26632	0.02
9.315	-0.26725	0.02
9.325	-0.26677	0.02
9.335	-0.26624	0.02
9.345	-0.26573	0.02
9.355	-0.26521	0.02
9.365	-0.26522	0.02
9.375	-0.26588	0.02
9.385	-0.26575	0.02
9.395	-0.265	0.02
9.405	-0.26453	0.02
9.415	-0.26539	0.02
9.425	-0.26576	0.02
9.435	-0.26508	0.02
9.445	-0.26514	0.02
9.455	-0.26592	0.02
9.465	-0.26664	0.02
9.475	-0.26721	0.02
9.485	-0.26749	0.02
9.495	-0.26842	0.02
9.505	-0.26908	0.02
9.515	-0.27005	0.02
9.525	-0.27084	0.02
9.535	-0.27006	0.02
9.545	-0.26899	0.02
9.555	-0.26936	0.02

9.565	-0.26775	0.02
9.575	-0.26719	0.02
9.585	-0.26637	0.02
9.595	-0.2656	0.02
9.605	-0.26488	0.02
9.615	-0.26337	0.02
9.625	-0.26314	0.02
9.635	-0.262	0.02
9.645	-0.26068	0.02
9.655	-0.25964	0.02
9.665	-0.2589	0.02
9.675	-0.25821	0.02
9.685	-0.25741	0.02
9.695	-0.25624	0.02
9.705	-0.25447	0.02
9.715	-0.25291	0.02
9.725	-0.25243	0.02
9.735	-0.25282	0.02
9.745	-0.25219	0.02
9.755	-0.25106	0.02
9.765	-0.25057	0.02
9.775	-0.25019	0.02
9.785	-0.25024	0.02
9.795	-0.25086	0.02
9.805	-0.25106	0.02
9.815	-0.25187	0.02
9.825	-0.25403	0.02
9.835	-0.25714	0.02
9.845	-0.25769	0.02
9.855	-0.25924	0.02
9.865	-0.26042	0.02
9.875	-0.26127	0.02
9.885	-0.2615	0.02
9.895	-0.26047	0.02
9.905	-0.25954	0.02
9.915	-0.25948	0.02
9.925	-0.25966	0.02
9.935	-0.25936	0.02
9.945	-0.25895	0.02
9.955	-0.25897	0.02

9.965	-0.26071	0.02
9.975	-0.26369	0.02
9.985	-0.26358	0.02
9.995	-0.26308	0.02
10.005	-0.26475	0.02
10.015	-0.26467	0.02
10.025	-0.26409	0.02
10.035	-0.26407	0.02
10.045	-0.26543	0.02
10.055	-0.26736	0.02
10.065	-0.26808	0.02
10.075	-0.26708	0.02
10.085	-0.26513	0.02
10.095	-0.26189	0.02
10.105	-0.25777	0.02
10.115	-0.2539	0.02
10.125	-0.25075	0.02
10.135	-0.2489	0.02
10.145	-0.24651	0.02
10.155	-0.24452	0.02
10.165	-0.24461	0.02
10.175	-0.2446	0.02
10.185	-0.24497	0.02
10.195	-0.24553	0.02
10.205	-0.24658	0.02
10.215	-0.24813	0.02
10.225	-0.24988	0.02
10.235	-0.25173	0.02
10.245	-0.25301	0.02
10.255	-0.25459	0.02
10.265	-0.2554	0.02
10.275	-0.25557	0.02
10.285	-0.2551	0.02
10.295	-0.25489	0.02
10.305	-0.25361	0.02
10.315	-0.25256	0.02
10.325	-0.24929	0.02
10.335	-0.24704	0.02
10.345	-0.24702	0.02
10.355	-0.24717	0.02

10.365 -0.24701 0.02

10.375 -0.2461 0.02

10.385 -0.24624 0.02

10.395 -0.24468 0.02

10.405 -0.24328 0.02

10.415 -0.24138 0.02

10.425 -0.23929 0.02

10.435 -0.23882 0.02

10.445 -0.23617 0.02

10.455 -0.23443 0.02

10.465 -0.23309 0.02

10.475 -0.23171 0.02

10.485 -0.23064 0.02

10.495 -0.22984 0.02

10.505 -0.22882 0.02

10.515 -0.228 0.02

10.525 -0.22647 0.02

10.535 -0.22302 0.02

10.545 -0.22134 0.02

10.555 -0.22047 0.02

10.565 -0.22036 0.02

10.575 -0.21964 0.02

10.585 -0.21817 0.02

10.595 -0.21696 0.02

10.605 -0.21599 0.02

10.615 -0.21547 0.02

10.625 -0.21524 0.02

10.635 -0.21434 0.02

10.645 -0.21301 0.02

10.655 -0.21236 0.02

10.665 -0.21194 0.02

10.675 -0.21131 0.02

10.685 -0.21131 0.02

10.695 -0.21107 0.02

10.705 -0.2101 0.02

10.715 -0.20955 0.02

10.725 -0.20951 0.02

10.735 -0.21085 0.02

10.745 -0.21216 0.02

10.755 -0.21354 0.02

10.765 -0.21422 0.02

10.775 -0.21347 0.02

10.785 -0.21277 0.02

10.795 -0.21239 0.02

10.805 -0.21186 0.02

10.815 -0.21192 0.02

10.825 -0.21288 0.02

10.835 -0.21344 0.02

10.845 -0.2147 0.02

10.855 -0.21508 0.02

10.865 -0.21521 0.02

10.875 -0.21556 0.02

10.885 -0.21586 0.02

10.895 -0.21655 0.02

10.905 -0.21669 0.02

10.915 -0.21571 0.02

10.925 -0.21442 0.02

10.935 -0.21204 0.02

10.945 -0.21041 0.02

10.955 -0.20882 0.02

10.965 -0.20836 0.02

10.975 -0.20836 0.02

10.985 -0.20874 0.02

10.995 -0.20932 0.02

11.005 -0.20954 0.02

11.015 -0.20873 0.02

11.025 -0.20841 0.02

11.035 -0.20768 0.02

11.045 -0.20698 0.02

11.055 -0.20576 0.02

11.065 -0.20438 0.02

11.075 -0.2034 0.02

11.085 -0.20207 0.02

11.095 -0.20113 0.02

11.105 -0.2008 0.02

11.115 -0.20005 0.02

11.125 -0.20006 0.02

11.135 -0.20049 0.02

11.145 -0.20058 0.02

11.155 -0.20067 0.02

11.165 -0.20128 0.02

11.175 -0.20131 0.02

11.185 -0.20095 0.02

11.195 -0.19978 0.02

11.205 -0.19862 0.02

11.215 -0.19795 0.02

11.225 -0.19582 0.02

11.235 -0.1941 0.02

11.245 -0.19264 0.02

11.255 -0.19104 0.02

11.265 -0.19075 0.02

11.275 -0.19047 0.02

11.285 -0.19022 0.02

11.295 -0.18999 0.02

11.305 -0.18939 0.02

11.315 -0.1883 0.02

11.325 -0.18742 0.02

11.335 -0.18671 0.02

11.345 -0.18563 0.02

11.355 -0.18438 0.02

11.365 -0.1834 0.02

11.375 -0.18287 0.02

11.385 -0.18348 0.02

11.395 -0.18322 0.02

11.405 -0.18363 0.02

11.415 -0.18352 0.02

11.425 -0.18316 0.02

11.435 -0.18267 0.02

11.445 -0.18216 0.02

11.455 -0.18071 0.02

11.465 -0.18025 0.02

11.475 -0.17928 0.02

11.485 -0.17823 0.02

11.495 -0.17786 0.02

11.505 -0.17711 0.02

11.515 -0.17632 0.02

11.525 -0.17535 0.02

11.535 -0.17419 0.02

11.545 -0.17309 0.02

11.555 -0.17151 0.02

11.565 -0.16976 0.02

11.575 -0.16819 0.02

11.585 -0.16729 0.02

11.595 -0.16624 0.02

11.605 -0.1658 0.02

11.615 -0.16645 0.02

11.625 -0.16794 0.02

11.635 -0.1682 0.02

11.645 -0.16774 0.02

11.655 -0.16671 0.02

11.665 -0.16592 0.02

11.675 -0.16527 0.02

11.685 -0.16329 0.02

11.695 -0.1625 0.02

11.705 -0.16162 0.02

11.715 -0.16085 0.02

11.725 -0.15937 0.02

11.735 -0.15776 0.02

11.745 -0.15761 0.02

11.755 -0.15802 0.02

11.765 -0.15751 0.02

11.775 -0.15695 0.02

11.785 -0.15647 0.02

11.795 -0.15595 0.02

11.805 -0.15563 0.02

11.815 -0.15529 0.02

11.825 -0.15472 0.02

11.835 -0.15462 0.02

11.845 -0.15405 0.02

11.855 -0.15365 0.02

11.865 -0.15374 0.02

11.875 -0.15399 0.02

11.885 -0.15413 0.02

11.895 -0.1543 0.02

11.905 -0.15308 0.02

11.915 -0.15161 0.02

11.925 -0.15174 0.02

11.935 -0.15041 0.02

11.945 -0.14979 0.02

11.955 -0.14981 0.02

11.965 -0.14974 0.02

11.975 -0.1495 0.02

11.985 -0.14887 0.02

11.995 -0.14928 0.02

12.005 -0.14892 0.02

12.015 -0.14763 0.02

12.025 -0.14596 0.02

12.035 -0.145 0.02

12.045 -0.14495 0.02

12.055 -0.14437 0.02

12.065 -0.14376 0.02

12.075 -0.14455 0.02

12.085 -0.14463 0.02

12.095 -0.1441 0.02

12.105 -0.14369 0.02

12.115 -0.14294 0.02

12.125 -0.14256 0.02

12.135 -0.14224 0.02

12.145 -0.14219 0.02

12.155 -0.14207 0.02

12.165 -0.14171 0.02

12.175 -0.14192 0.02

12.185 -0.14222 0.02

12.195 -0.14223 0.02

12.205 -0.14158 0.02

12.215 -0.14108 0.02

12.225 -0.13966 0.02

12.235 -0.13816 0.02

12.245 -0.13889 0.02

12.255 -0.13824 0.02

12.265 -0.13692 0.02

12.275 -0.13686 0.02

12.285 -0.1359 0.02

12.295 -0.13512 0.02

12.305 -0.13428 0.02

12.315 -0.13377 0.02

12.325 -0.1336 0.02

12.335 -0.134 0.02

12.345 -0.13281 0.02

12.355 -0.13213 0.02

12.365 -0.13065 0.02

12.375 -0.13012 0.02

12.385 -0.12988 0.02

12.395 -0.12951 0.02

12.405 -0.12998 0.02

12.415 -0.13023 0.02

12.425 -0.12985 0.02

12.435 -0.13009 0.02

12.445 -0.1295 0.02

12.455 -0.12961 0.02

12.465 -0.12967 0.02

12.475 -0.12911 0.02

12.485 -0.12787 0.02

12.495 -0.12782 0.02

12.505 -0.1283 0.02

12.515 -0.12779 0.02

12.525 -0.12706 0.02

12.535 -0.12706 0.02

12.545 -0.12663 0.02

12.555 -0.12603 0.02

12.565 -0.12539 0.02

12.575 -0.12432 0.02

12.585 -0.12333 0.02

12.595 -0.12223 0.02

12.605 -0.12161 0.02

12.615 -0.12126 0.02

12.625 -0.12116 0.02

12.635 -0.12033 0.02

12.645 -0.11953 0.02

12.655 -0.11872 0.02

12.665 -0.1177 0.02

12.675 -0.1168 0.02

12.685 -0.11597 0.02

12.695 -0.11519 0.02

12.705 -0.11407 0.02

12.715 -0.11278 0.02

12.725 -0.11167 0.02

12.735 -0.11178 0.02

12.745 -0.11197 0.02

12.755 -0.11249 0.02

12.765 -0.11219 0.02

12.775 -0.11181 0.02

12.785 -0.11139 0.02

12.795 -0.11097 0.02

12.805 -0.11056 0.02

12.815 -0.1106 0.02

12.825 -0.11026 0.02

12.835 -0.10941 0.02

12.845 -0.1089 0.02

12.855 -0.10852 0.02

12.865 -0.10701 0.02

12.875 -0.10628 0.02

12.885 -0.10473 0.02

12.895 -0.10372 0.02

12.905 -0.10314 0.02

12.915 -0.10258 0.02

12.925 -0.10235 0.02

12.935 -0.10072 0.02

12.945 -0.09956 0.02

12.955 -0.097941 0.02

12.965 -0.096634 0.02

12.975 -0.095703 0.02

12.985 -0.094906 0.02

12.995 -0.094713 0.02

13.005 -0.093085 0.02

13.015 -0.091967 0.02

13.025 -0.09114 0.02

13.035 -0.089556 0.02

13.045 -0.088245 0.02

13.055 -0.087464 0.02

13.065 -0.08639 0.02

13.075 -0.086118 0.02

13.085 -0.086172 0.02

13.095 -0.085443 0.02

13.105 -0.084728 0.02

13.115 -0.083874 0.02

13.125 -0.082983 0.02

13.135 -0.082465 0.02

13.145 -0.082056 0.02

13.155 -0.082714 0.02

13.165 -0.082111 0.02

13.175 -0.080967 0.02

13.185 -0.079565 0.02

13.195 -0.078436 0.02

13.205 -0.077619 0.02

13.215 -0.076114 0.02

13.225 -0.075436 0.02

13.235 -0.074117 0.02

13.245 -0.07209 0.02

13.255 -0.070778 0.02

13.265 -0.069859 0.02

13.275 -0.069468 0.02

13.285 -0.069051 0.02

13.295 -0.068155 0.02

13.305 -0.067378 0.02

13.315 -0.065467 0.02

13.325 -0.063504 0.02

13.335 -0.063217 0.02

13.345 -0.061753 0.02

13.355 -0.059849 0.02

13.365 -0.058457 0.02

13.375 -0.057523 0.02

13.385 -0.056536 0.02

13.395 -0.055712 0.02

13.405 -0.055382 0.02

13.415 -0.054738 0.02

13.425 -0.053066 0.02

13.435 -0.051371 0.02

13.445 -0.049116 0.02

13.455 -0.047492 0.02

13.465 -0.044978 0.02

13.475 -0.044146 0.02

13.485 -0.044763 0.02

13.495 -0.043818 0.02

13.505 -0.043784 0.02

13.515 -0.044443 0.02

13.525 -0.042575 0.02

13.535 -0.040053 0.02

13.545 -0.037716 0.02

13.555 -0.035524 0.02

13.565 -0.033925 0.02

13.575 -0.031154 0.02

13.585 -0.028748 0.02

13.595 -0.025339 0.02

13.605 -0.020233 0.02

13.615 -0.01588 0.02

13.625 -0.013257 0.02

13.635 -0.009315 0.02

13.645 -0.005396 0.02

13.655 0.001059 0.02

13.665 0.006407 0.02

13.675 0.011382 0.02

13.685 0.015816 0.02

13.695 0.021006 0.02

13.705 0.022703 0.02

13.715 0.028753 0.02

13.725 0.032501 0.02

13.735 0.036243 0.02

13.745 0.041064 0.02

13.755 0.046854 0.02

13.765 0.052741 0.02

13.775 0.057284 0.02

13.785 0.061792 0.02

13.795 0.065754 0.02

13.805 0.069385 0.02

13.815 0.074564 0.02

13.825 0.078777 0.02

13.835 0.083556 0.02

13.845 0.087427 0.02

13.855 0.092533 0.02

13.865 0.096648 0.02

13.875 0.10008 0.02

13.885 0.10335 0.02

13.895 0.10876 0.02

13.905 0.11297 0.02

13.915 0.11817 0.02

13.925 0.1235 0.02

13.935 0.12831 0.02

13.945 0.13451 0.02

13.955 0.13801 0.02

13.965 0.14143 0.02

13.975 0.14482 0.02

13.985 0.14835 0.02

13.995 0.15235 0.02

14.005 0.15593 0.02

14.015 0.15983 0.02

14.025 0.16443 0.02

14.035 0.16862 0.02

14.045 0.17333 0.02

14.055 0.17679 0.02

14.065 0.18022 0.02

14.075 0.18306 0.02

14.085 0.18514 0.02

14.095 0.1863 0.02

14.105 0.18688 0.02

14.115 0.18823 0.02

14.125 0.189 0.02

14.135 0.18824 0.02

14.145 0.18694 0.02

14.155 0.18532 0.02

14.165 0.18255 0.02

14.175 0.17947 0.02

14.185 0.17562 0.02

14.195 0.16913 0.02

14.205 0.1624 0.02

14.215 0.15643 0.02

14.225 0.14943 0.02

14.235 0.14387 0.02

14.245 0.13814 0.02

14.255 0.13131 0.02

14.265 0.12358 0.02

14.275 0.11618 0.02

0 -0.912

1.1766 -0.912

1.595 -0.809

3.35 -0.377

3.53 -0.697

14.245 -0.00697

14.275 0.11618